Optimal sizing and Placement of Static Var Compensator for Voltage Stability Enhancement in Radial Distribution Network using Particle Swarm Optimization

(Case Study: Gefersa Substation Outgoing Feeder**)**

Gadissa Fikru Hundessa

A Thesis Submitted to the Department of Electrical Power and Control Engineering

School of Electrical Engineering and Computing

Presented in Partial Fulfillment of the Requirement for the Degree of Master's in Electrical Power and Control Engineering

(Power System Engineering)

Office of Graduate Studies

Adama Science and Technology University

September, 2024

Adama, Ethiopia

Optimal sizing and Placement of Static Var Compensator for Voltage Stability Enhancement in Radial Distribution Network using Particle Swarm Optimization

Gadissa Fikru Hundessa

Advisor: Dr.CS Reddy

A Thesis Submitted to the Department of Electrical Power and Control Engineering

School of Electrical Engineering and Computing

Presented in Partial Fulfillment of the Requirement for the Degree of Master’s in Electrical Power and Control Engineering

(Power System Engineering)

Office of Graduate Studies

Adama Science and Technology University

September, 2024

Adama, Ethiopia

DECLARATION

I, hereby declare that this Master Thesis entitled **“Optimal sizing and Placement of Static Var Compensator for Voltage Stability Enhancement in Radial Distribution Network using Particle Swarm Optimization”** is my original work. That is, it has not been submitted for the award of any academic degree, diploma, or certificate in any other university. All sources of materials that are used for this thesis have been duly acknowledged through citation.

Gadissa Fikru Hundessa	____________________	_____________
Name of student	Signature	Date

RECOMMENDATION

I, the advisor of this thesis, hereby certify that I have read the revised version of the thesis entitled "**Optimal sizing and Placement of Static Var Compensator for Voltage Stability Enhancement in Radial Distribution Network using Particle Swarm Optimization"** prepared under my guidance by Gadissa Fikru Hundessa submitted in partial fulfillment of the requirements for the degree of Masters of Science in Electrical Power and Control Engineering (Power System Engineering). Therefore, I recommend the submission of a revised version of the thesis to the department following the applicable procedures.

____________________	____________________	_____________
Advisor	Signature	Date

APPROVAL PAGE

I, the advisor of the thesis entitled "**Optimal sizing and Placement of Static Var Compensator for Voltage Stability Enhancement in Radial Distribution Network using Particle Swarm Optimization''** and developed by Gadissa Fikru Hundessa, hereby certify that the recommendation and suggestions made by the board of examiners are appropriately incorporated into the final version of the thesis.

______________________	______________________	_______________
Advisor	Signature	Date

We, the undersigned, members of the Board of Examiners of the thesis by Gadissa Fikru Hundessa have read and evaluated the thesis entitled "**Optimal sizing and Placement of Static Var Compensator for Voltage Stability Enhancement in Radial Distribution Network using Particle Swarm Optimization"** and examined the candidate during the open defense. This is, therefore, to certify that the thesis is accepted for partial fulfillment of the requirement of the degree of Master of Science in Electrical Power and Control Engineering (Power System Engineering).

____________________	_______________	______________
Chairperson	Signature	Date
____________________	_______________	______________
Internal Examiner	Signature	Date
Dr. Wondwossen Astatike	_______________	______________
External Examiner	Signature	Date

Finally, approval and acceptance of the thesis is contingent upon submission of its final copy to the Office of Postgraduate Studies (OPGS) through the Department Graduate Council (DGC) and School Graduate Committee (SGC).

______________________	_______________	______________
Department Head	Signature	Date
______________________	_______________	______________
School Dean	Signature	Date
______________________	_______________	______________
Office of Graduate Studies, Dean	Signature	Date

ACKNOWLEDGMENTS

First and for most, I want to deserve all the glory and honor to the living God, Christ of Jesus.
Secondly, following to this my warmest thanks go to my Advisor Dr.CS Reddy, for your professional advice, critical and constructive comments, clear guidance and suggestions in shaping my research paper in this form. Indeed, your respect and patience is unforgettable!
And also, I would like to thank to those who helped in providing the data used in this thesis, mainly Mr.Bonsa, Mr.Inchala Itefa memebes of EEP Gefersa Substation and EEU staff for their cooperation for providing all the necessary data that are helpful to complete this thesis.
Finally, I would like to thank all my families, best friends, who have contributed in different ways and those of you who have helped me in completing my studies.

TABLE OF CONTENTS

LIST OF TABLES

TABLES PAGE

LIST OF FIGURES AND ILLUSTRATIONS

FIGURES PAGE

LIST OF ACRONYMS AND ABBREVIATIONS

AC	Alternative Current
AI	Artificial intelligence
ALOA	Ant Lion Optimization Algorithm
BCBV	Branch-Current to Bus Voltage
BESS	Battery Energy Storage System
BIBC	Bus injection to Branch Current
DC	Direct Current
DE	Differential Evolution
D-STATCOM	Distribution Static Synchronous compensator
D-SSSC	Distribution Static Synchronous Series compensator
D-UPFC	Distribution Unified Power Flow Controller
D-TCSC	Distribution Thyristor Controlled Series Compensator
D-GPSFC	Distribution Green Plug System Flow Control
D-SFC	Distribution Switched Filter Compensation
ETAP	Electrical Transient and Analysis Program
FACTS	Flexible AC Transmission System
FBS	Forward/Backward Sweep
GA	Genetic Algorithm
HVDC	High Voltage Direct Current
IPC	Interphase power controller
IPFC	Interline Power Flow Control
OPF	Optimal Power Flow
PSO	Particle Swarm Optimization
SVC	Static Var Compensator
SSSC	Static Synchronous Series Compensator
STATCOM	Static Synchronous Compensator
TCPAR	Thyristor Controlled Phase Angle Regulator
TCSC	Thyristor Controlled Series Compensators
TCR	Thyristor Controlled Reactor
TCSR	Thyristor Controlled Series Reactor

TSC	Thyristor Switched Capacitor
TSSC	Thyristor Switched Series Capacitor
TSSR	Thyristor Switched Series Reactor
TCBR	Thyristor Control Breaking Resistor
SMESS	Superconducting Magnetic Energy Storage
UPFC	Unified Power Flow Controller

ABSTRACT

Urbanization and the ongoing rise in power consumption necessitate the use of a dependable and high-quality power supply system. Unfortunately, a number of issues have arisen with the current power distribution system, making it unable to securely and dependably provide the growing demand for power. Power loss, a poor voltage profile, significant power interruptions, distorted voltage and current at the customer end, and unstable voltage in the system node are the primary issues in the distribution system that affects performance. The performance of the distribution was enhanced by utilizing the appropriate size and positioning of the SVC. The Gefersa 14 outgoing feeder, which is part of the Gefersa distribution network, is the subject of the study. In order to assess power loss and voltage profile of the chosen feeder, the Backward-Forward Sweep (BFS) method implemented in MATLAB has been modeled and load flow analysis conducted.

Multi objective function was formulated in this thesis including voltage profile, real and reactive power loss by using appropriate sizing and positioning of SVC using PSO. By using optimal power flow backward/forward load flow analysis at base case the power loss and the voltage of each bus is obtained. From the result of base case real and reactive power loss are 401.432 KW and 350.081 respectively and 41 buses are below the IEEE standard level, the bus selected for SVC connection is at bus 82. By using appropriate size and location of SVC with PSO the size is 2500.51KVAr and connected at bus 82. After integration of static Var compensator real and reactive power loss is reduced to 229.208kw and 216.722kvar respectively. Following this integration, the feeder's real and reactive power loss was reduced by 43% and 38% respectively, resulting in an annual cost reduction of 4,828,929.37 *birr for energy loss. This demonstrates that SVC is integrated in the feeder at the optimal size and placement; 3,628,359.72 birr may be saved annually.*

Keywords: *Static Var compensator, particle swarm optimization, Backward/Forward load flow sweep, Voltage Profile, MATLAB,Power Loss*

CHAPTER ONE

1.INTRODUCTION

1.1 Background

The primary components of the electrical power industry's system are electrical power generation, transmission, and distribution. The process of moving electrical energy from its source to its consumer involves a number of complications, including changes in the weather, a generation deficit relative to demand, breakdowns, and variations in the connected load on the line. Modern commercial and industrial equipment is extremely sensitive to issues with power quality (Kasari et al., 2017). Customers in the business and industrial sectors depend more and more on reliable, high-quality electricity. Failures and switching operations in the network can lead to transients, interruptions, and voltage instability. Additionally, loads that produce flicker, or rapid voltage changes, harmonics, and phase imbalance, can also cause insufficient power quality. In large distribution networks, the most frequent disruptions that negatively affect electric customer process activities are momentary voltage sags and interruptions. Customers and utilities may become more conscious of power quality as a result of the growing need for dependable, high-quality electricity and the rise in distorting loads (Katariya & Shriwastava, 2017). Power systems of days run close to their limits because of the ongoing rise in demand. Constraint violations are mostly caused by voltage instability, which is also linked to voltage collapse and voltage stability, which are both related to reactive power control. Due to the increased transmission system flexibility, the Flexible AC Transmission System (FACTS) is now able to govern reactive power flow more dynamically (Nascimento & Gouvêa, 2017). System failure can also be caused by voltage instability, which can lead to generation tripping. The incapacity to meet the reactive power demand is the primary cause of voltage instability issues in power systems. Voltage profile is impacted when the system is unstable, and any decline in voltage profile is matched by an increase in the demand for reactive power. If the need for reactive power is not satisfied, the bus voltage will continue to drop, which could impair the system's ability to transfer power and could cause damage to or malfunction in the equipment (Adebisi et al., 2017).

Voltage instability is caused by distribution systems' high R/X ratio, which also contributes to excessive power loss. Shunt capacitors and series voltage regulators are the two traditional methods used to keep the distribution system's voltages within a reasonable range. However, these devices have certain drawbacks. Firstly, because typical series voltage regulators operate in steps, they are unable to provide reactive power and have a relatively slow response time. Shunt capacitors have the drawback of not being able to provide reactive power that is continuously varying. FACTS devices are utilized in order to address these issues (Dhanalakshmi, 2022). To achieve the needed goal like reducing power losses, raising the voltage profile and mitigating reactive power optimal sizing and positioning of FACTS devices are necessary. Researchers have proposed a variety of optimization techniques to size and place devices in the distribution network optimally in order to address power quality concerns and enhance performance.

Two method is there for placement and sizing FACTS in the distribution network. One of the approach is predicated based on conventional techniques including repeating load flows, sensitivity factor, and optimal power flow (OPF). Artificial intelligence (AI) algorithms like the Teaching and Learning Process (TLPOA), Particle Swarm Optimization (PSO), BFOA, DE,ACO, ALOA,GA HSOA,TS, and BA are used in the second method (Herwan & Mustaffa, 2022).

The Distribution Static Var Compensator, a shunt-connected device for injecting reactive power, is employed in this work. To determine the ideal location and size of SVC, an approach known as particle swarm optimization is employed. PSO is the most widely used algorithm among those mentioned above because of its quick convergence, low processing load, and simplicity of development.

In this thesis work, the MATLAB program and the PSO algorithm have been used to identify the proper sizing and positioning of SVC. Additionally, PSO has been used to determine the suitable candidate bus for SVC placement, with SVC being inserted at each bus with the corresponding size found by taking into account voltage profile enhancement and total loss reduction.

The MATLAB program's power flow analysis of the system makes use of the FBS load flow method. In order to lower real and reactive losses, improve the voltage profile, and stabilize the voltage of the distribution network, the SVC is thought to be implemented in the primary distribution system.

1.2 Statement of the Problem

Since voltage stability guarantees that customers will receive their electricity on time, it is an essential component of power system management and planning. However, there are a number of variables that can affect power systems and cause voltage instability, including high loads, reactive power requirements, and system emergencies. As a result, efficient techniques to improve voltage stability and preserve a safe power source must be developed. series voltage regulators are the traditional methods used to keep the distribution system's voltages within a reasonable range.

However, this device has certain drawbacks. Firstly, because typical series voltage regulators operate in steps, they are unable to provide reactive power and have a relatively slow response time. Voltage variations and possible voltage collapse may arise from this restriction, which may lead to an inefficient distribution of reactive power supply.

In this thesis project, the Gefersa distribution feeder had been chosen for this study. The Gefersa substation is located in the northern part of Ethiopia's capital, Addis Ababa, where a number of residential, commercial, and industrial centers are situated. This area is where the majority of the country's electricity is consumed. Sixteen distribution feeders on the substation serve electricity to different areas of Sheger City, including the burayu sub-city.

Due to the construction of several industries around ever-increasing residential and commercial buildings, and growing residential areas, load demand is continuously rising. The distribution network's growing load demand overloads the system component, resulting in power outages, losses, unstable voltage and lower voltage. The outgoing feeder in the Gefersa substation currently frequently encounters power disruptions due to the overloading of the current system, which causes power loss and various bus voltage levels to operate close to the permitted voltage limit.

By looking at the control room's current distribution system condition and the data that was recorded, this issue was found. The thesis work has focused on one of the outgoing feeders of the Gefersa substation, which is occasionally overloaded and experiences power interruptions. The Gefersa substation's outgoing feeder-14 has been selected as a case study as a result. An appropriate fix was applied to the outgoing feeder-14 of the Gefersa substation in order to resolve the problems. The resolution of the highlighted problem has been largely attributed to the utilization of the PSO algorithm for the incorporation of SVC to the chosen bus with appropriate placement and size.

1.3 Objective

1.3.1 General Objective

The general objective of the thesis was by using PSO to optimize the size and location of the SVC in order to maximize voltage stability, decrease power loss, minimize voltage deviations, and assure reliable power system operation.

1.3.2 Specific Objectives

- Modeling of the distribution system for the selected feeder
- Analyze the existing distribution voltage profile and power loss based on BFS load flow method.
- Formulate a multi-objective function taking into consideration of real and reactive power loss and voltage profile after Integration of compensating devices.
- Analyze optimal allocation and capacity of SVC using particle swarm optimization algorithm.
- Compare the existing distribution voltage profile and power loss with the after integration of Static Var Compensator.

1.4 Scope and Limitation of the Study

Determine the critical buses in the radial distribution substation feeder by analyzing the load flow results. Take into account variables like voltage deviations, reactive power consumption, or other stability indicators to find the critical buses that are vulnerable to voltage instability or have low voltage margins. Next, calculate the static Var compensator size using the particle swarm optimization algorithm to inject the proper amount of reactive power into the radial distribution feeder buses. In order to guarantee that voltage deviations are reduced and voltage stability is improved within the radial distribution feeder buses, the findings of the analysis are finally analyzed following the ideal placement and sizing of the static Var compensator.

The thesis doesn't look at how the device performs in a dynamic operating state. Furthermore, this thesis ignores phase imbalance and the harmonic effect.

1.5 Significance of the Study

Voltage collapse, in which portion of the distribution feeder experiences a sharp reduction in voltage, can be caused by voltage instability. In order to minimize voltage collapse and maintain a steady voltage profile across the feeder, voltage instability can be reduced by injecting reactive power through the SVC. Using an SVC to improve voltage stability helps keep voltage levels along the distribution substation feeder within allowable bounds. By doing this, the chance of damage or failure from voltage fluctuations is reduced and the electrical appliances and equipment connected to the feeder are guaranteed to receive a steady and consistent voltage. Additionally, voltage regulation, power transfer capability, system dependability, and cost-effectiveness are all improved when a distribution substation feeder's SVC is sized and positioned optimally employing particle swarm optimization for voltage stability enhancement.

1.6 Organization of the Study

The five parts that make up this thesis work's content are ordered as follows.

The thesis work's general introduction, which explains the main idea and provides guidance for the thesis's body, is presented in the first chapter. The second chapter provides an overview of FACTS devices, the theoretical foundation of the distribution system, and a way for enhancing system performance. It includes an analysis of the literature related to the quality of power issue with the distribution system, specifically with regard to lowering power loss and enhancing the distribution line's voltage profile. In the third chapter, the case study region is described, the necessary data is gathered and analyzed, and optimization approaches are covered. Chapter Four presents the simulation findings, a cost-benefit analysis, and a discussion of the appropriate size and placement of the SVC of the Gefersa outgoing feeder-14 after and before incorporation of SVC. Final part contains the thesis work's conclusions and recommendations.

CHAPTER TWO

2. LITERATURES REVIEW

2.1 Electrical Power System Network

The three main parts of an electric power system are the distribution, transmission, and generation systems. Power plants are positioned to produce power in a strategic manner, frequently far from consumers. They are then moved across great distances to load centers via transmission lines, which are conductors. Ultimately, a distribution network is used to distribute power to the end users. Primary network lines carry the medium voltage to transformers close to the around customers. Secondary network lines are used to distribute the voltage to a large number of consumers after distribution transformers lower it to a level appropriate for household appliances.

Lastly, a distribution network is employed to connect with a variety of customers, both big and little. In most towns and villages, distribution networks are established throughout to supply power to each individual customer. The distribution system must be able to meet each customer's unique requirements, taking into account factors like power quality, efficiency, and energy demand. Distributors, feeders, and service mains are the most prevalent parts (Rosyadi et al., 2018).

2.2 Power System Stability

The ability of an electrical power system to sustain stable and suitable operating conditions in the face of disruptions or system modifications is referred to as power system stability. It entails keeping the ratio of generation to load in check and making sure that frequencies and voltages stay stable within allowable bounds. A power system's stability is essential to its dependable and secure functioning. Several stability problems may surface in the event of system disturbances, such as faults, abrupt changes in load, or loss of generation. Unwanted outcomes like frequency fluctuations, voltage collapse, or even widespread blackouts may result from these problems. Three factors can be used to categorize a power system's stability: rotor angle stability, frequency stability, and voltage stability (Hatziargyriou et al., 2021a).Classification of power system stability is shown in figure 2.1.

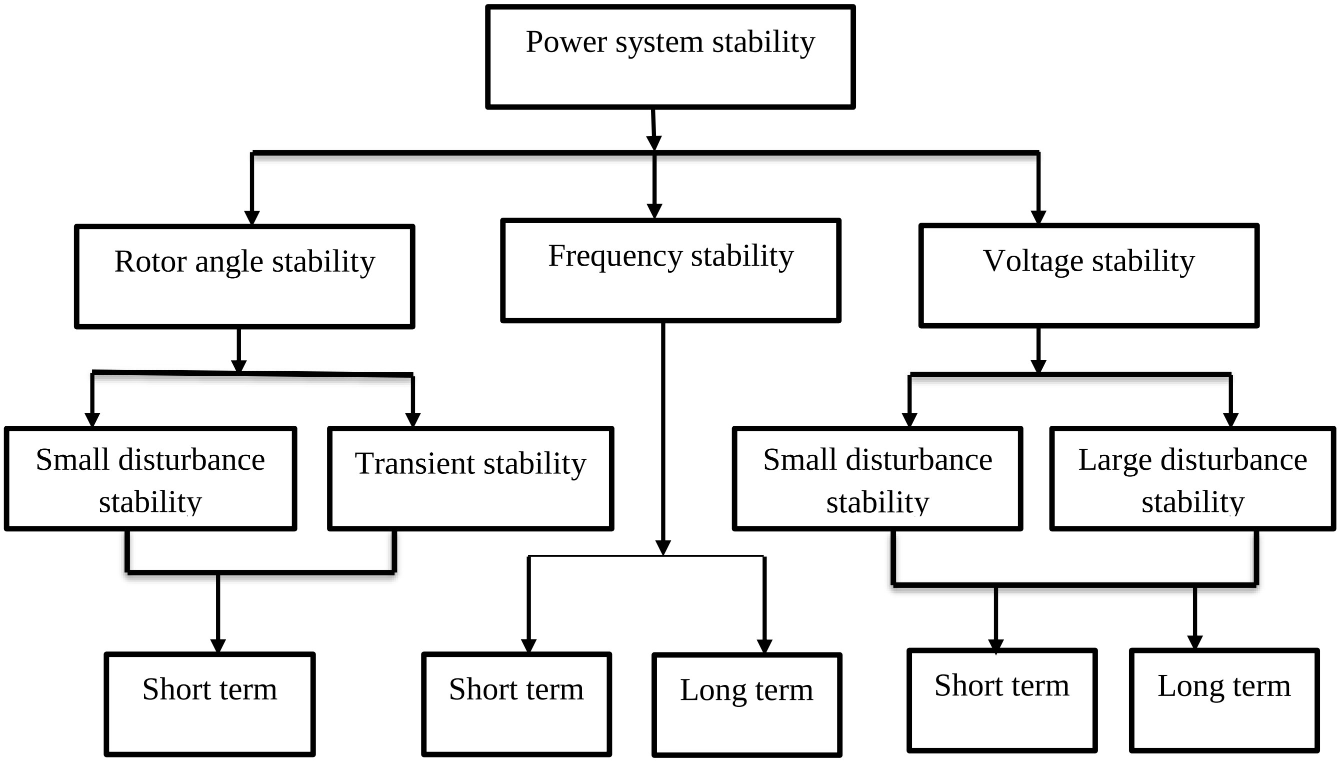

Figure 2.1 Classification of power system stability (Hatziargyriou et al., 2021b)

2.2.1 Rotor Angle Stability

Maintaining rotor attitude balance in an electrical system network requires the synchronization of interconnected synchronous machines. The analysis of electro-mechanical oscillations is the main focus of this problem. The synchronous device's power output modifications during rotor oscillation also referred to as either steady-state stability or transient state stability are a crucial factor in rotor angle stability(Song et al., 2020).

2.2.2 Frequency Stability

The ability of a power machine to sustain a steady frequency even following a significant disruption that results in a significant imbalance between generation and load is referred to as frequency stability. In order to minimize unintentional load loss and maintain or restore the balance between machine generation and load, it depends on community functionality. Issues with frequency balance are typically brought on by inadequate generating reserve, inadequate control and safety equipment coordination, or inadequate equipment reactions. Frequency stability can manifest as a phenomenon with a long duration or as a short-period event that lasts only a few seconds(Conte et al., 2020).

2.2.3 Voltage Stability

The strength system's capacity to sustain optimal voltage at all buses throughout regular operations and in the time of a disruption is referred to as voltage stability. On the other hand, voltage instability happens when a disturbance causes a slow decrease or rise in bus voltages. The inability of the power device to meet the demand for reactive strength is the main source of instability. This reactive energy can be supplied by generators via transmission networks, or it can be instantly compensated for at load buses through the use of FACTS and shunt capacitors. Reactive strength becomes more important in the presence of disturbances, malfunctions, and modifications to operating conditions. This sudden increase in power requires the electrical device to operate near to its maximum capacity, signaling high loading conditions. These situations might result in voltage collapse, which makes voltage stability a crucial issue that necessitates a suitable strategy to avoid machine failure (Wondie, 2022).

A. Large disturbance voltage stability

The term "large-disturbance voltage stability" describes a device's capacity to maintain high voltages during significant disturbances, such as system failures, data loss, or circuit emergencies. This could last anything from a few seconds to several minutes. Large-scale disturbance voltage stability can be investigated using load flow analysis in the long run and non-linear time domain simulations in the short run (Hatziargyriou et al., 2021a).

B. Small disturbance voltage stability

The term "small-disturbance voltage balance" refers to the device's capacity to maintain constant voltages in the face of slight disturbances, such as progressive changes in the machine load. Small disturbance analysis is often performed in a solid state with the electrical device linearized at a predetermined operating factor. There are two ways to designate voltage balance: according to how long they have improved (voltage stability over a long or short period of time)(Idris, 2023).

The term "small-disturbance voltage balance" refers to the device's capacity to maintain high voltages in the face of minute disturbances and gradual changes in system load. Small disturbance analysis is often carried out in a steady state, with the energy system linearized around a specific operating point. There are two ways to classify voltage stability: first, according to how long they have been stable (long-term period voltage stability) or short-term period voltage stability.

A. Short term voltage stability

Involves a quick prominence that occurs within a few seconds to fractions of a second. Even though it is advised to stop using this word to distinguish it from brief rotor angle stability, it is still used in some research studies as transient voltage stability. The rapid response of voltage controllers, such as automatic voltage regulators (AVRs), generators, and power electronics converters, such as flexible AC transmission devices (FACTS) or high voltage DC (HVDC) links, is often linked to short-term balance issues. It is necessary to solve appropriate differential equations for the evaluation.

B. Long term voltage stability

The method involves slower acting machinery, including load self-restoration or on-load tap changers. In addition, load shedding and shunt compensation switching are examples of delayed corrective control measures. The relevant study session could be for a few or many minutes. A number of variables, including transformer tap changers, static load characteristics, operator manual control actions, and automatic generation control, need to be considered in order to effectively predict long-term voltage stability.

2.3 Factors Influencing Voltage Stability

Reactive power use, transmission, and generation all have a significant impact on the voltage stability issue. In fact, the reactive power delivered is decreased and certain transmission lines are significantly burdened when major generation units are taken out of service owing to unusual operating conditions or disturbances]. The load voltages therefore drop as a result of the increased reactive power requirement. Eventually, voltage collapse and instability are the results of the process (Gadal et al., 2023). The following list of variables in figure 2.2 affects voltage stability.

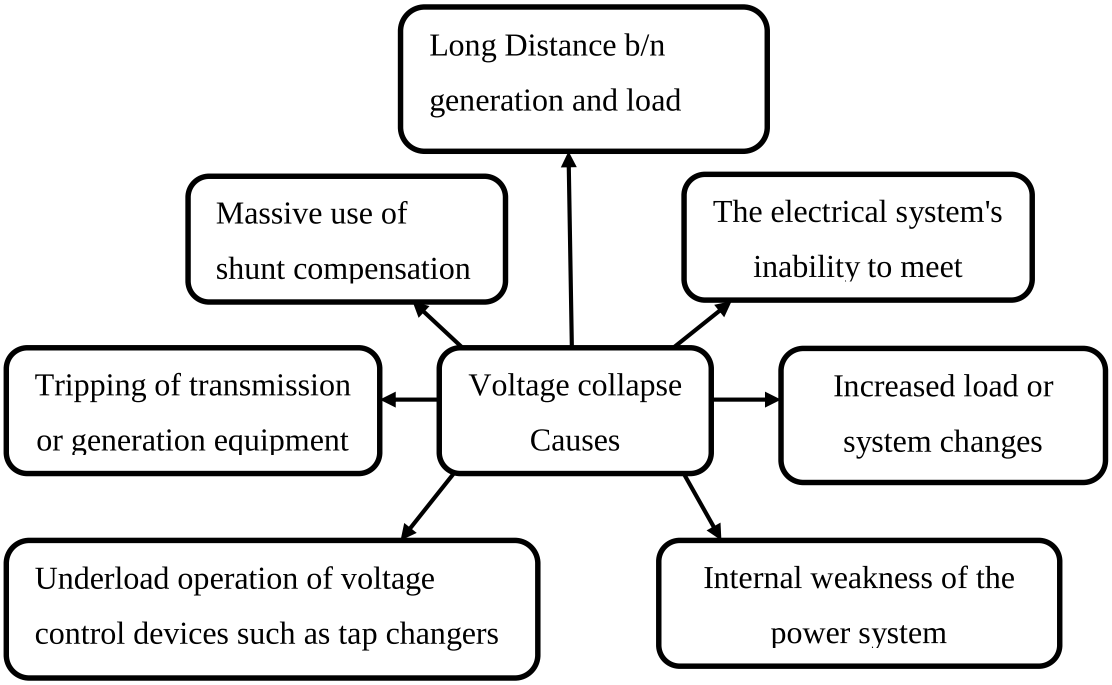

Figure 2.2 Voltage collapse causes (Niranjan et al., 2016).

2.4 Voltage Stability Prediction

For operators and academics, predicting and analyzing the voltage collapse phenomenon continues to be a significant issue. Within this framework, numerous investigations and scholars have concentrated on showcasing methodological techniques for the examination. These fall into two main categories: assessments of static and dynamic voltage stability. The dynamic components related to generation, transmission, distribution, and load are included in the dynamic analysis. It is distinguished by the intricacy of the calculations and data needed. In contrast, static analysis examines voltage stability mostly through load flow analyses. It includes an analysis of the equilibrium regime and enables us to determine the voltage levels and power transits via each of the system's busses and lines (Woldu et al., 2020).Method of voltage stability prediction is shown below in figure 2.3.

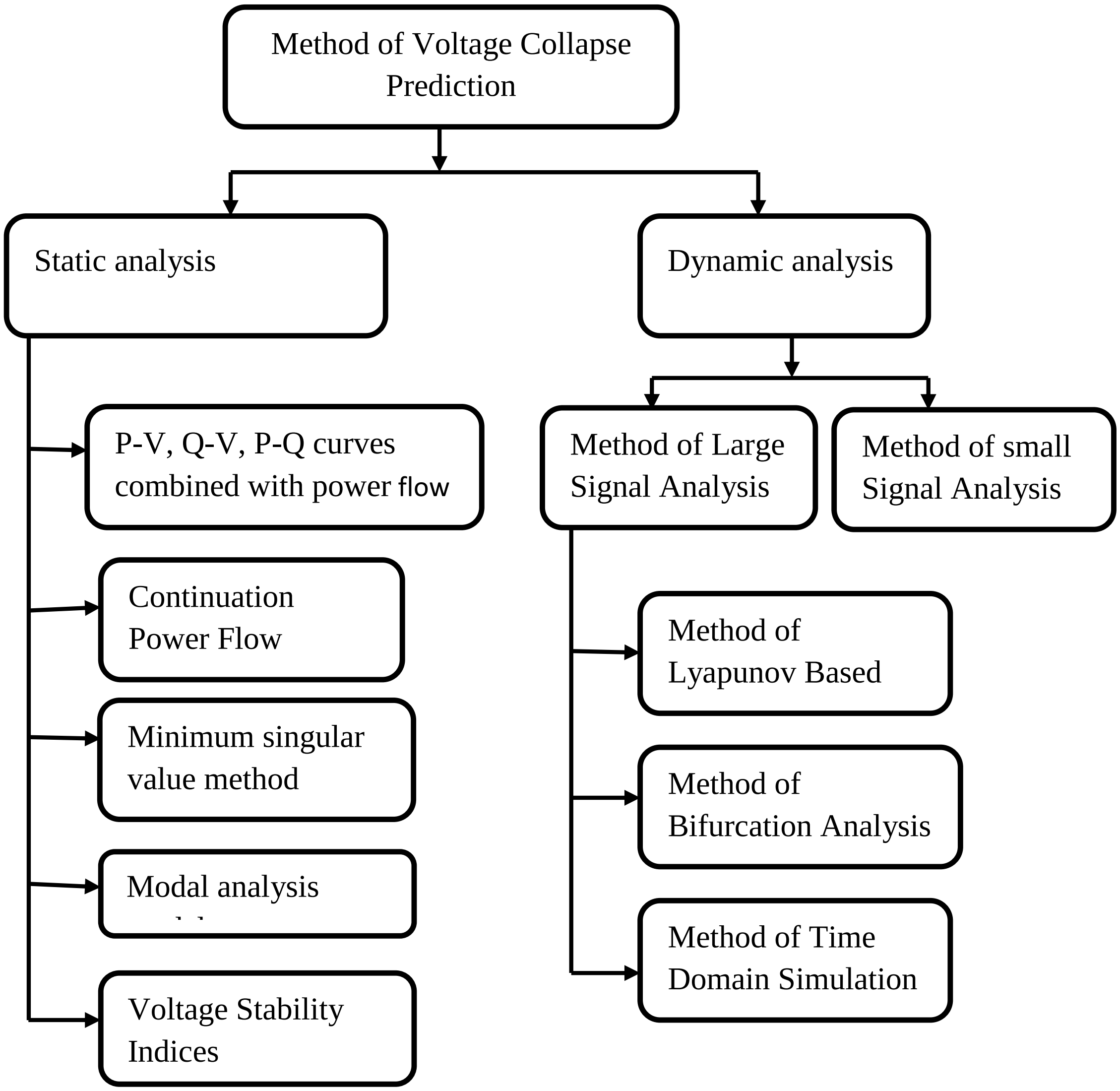

Figure 2.3 Method of Voltage Collapse Prediction(Asif et al., 2023)

2.5 Voltage Drop and Power Loss in the Distribution System

Although there are both technical and non-technical losses in electrical power distribution networks, industry wants efficient method to supply power at a good cost, with little voltage drop and power loss. The physical layout of the facilities and equipment in the power system, including the conductor, transformer, switches, and generators, results in copper loss, which is one of the technical losses connected to the distribution system.

The customer service procedure is the source of the non-technical losses; it involves erroneous metering and illegal use in coordination with utility employees. The distribution overhead cables' reactance and resistance are to blame for the voltage drop and power loss. While DG insertion, capacitor integration, network reconfiguration, and FACTS devices are some of the strategies that can reduce power loss and voltage drop, these problems are not easily resolved(Devi & Padma, 2017).

2.5.1 Technical Loss in Distribution Network

Technical losses in the power system are caused by the physical characteristics of the apparatuses. The most evident example is the power lost in transformers and transmission lines as a result of internal electrical resistance. Technical losses are those that happen organically (due to internal power system activity) and are mostly brought on by power dissipation in electrical system components including measuring systems, power transformers, transmission lines, and so forth. Technical losses in the power system in question can be calculated and controlled if the loads in it are known. Feeder losses, transformer losses, and substation losses are examples of technical losses that can happen during transmission and distribution. These comprise resistive losses in the main feeder, resistive losses in the secondary network, distribution transformer losses (resistive losses in the windings and core), resistive losses in the secondary network, resistive losses in the service drop, and losses from kWh meters.

There are inherent losses in the distribution of electricity that cannot be prevented. The following losses are examples of technical losses that are brought on by current passing over an electrical network: I^2R losses, which result from the finite resistance of conductors, are the source of copper losses in all inductors. The dielectric substance that makes conductor to separate and causes dielectric losses heats up and losses brought on by radiation and induction, which are brought on by the electromagnetic fields surrounding conductors. If there are known loads in the power system, then technical losses can be calculated and controlled (Memon et al., 2017).

2.5.2 Non-technical Loss in Distribution Network

Conversely, non-technical losses result from loads and situations that were not taken into account by the technical losses computation, or from events that happen outside of the power system. Since non-technical losses are not well documented and are often disregarded by device operators, they are more challenging to quantify. However, non-technical losses (NTL) are caused by power theft, inaccurate metering, unmeasured power, malfunctioning meters, disregarding past-due bills, bill which is not paid.

The difficulties that power suppliers encounter in managing NTLs have prompted the presentation of various strategies for the effective management of NTLs in energy distribution networks. The most efficient method for lowering NTLs right now is to use smart electronic meters. But even if they are favorable to install, they are expensive, and new infrastructure is required for data collection (Memon et al., 2017).

2.6 Load Flow Analysis in Radial Distribution Network

The planning, economical operation, and extension of power systems all depend heavily on load flow studies. They also play a key role in scheduling, improving current systems, and enabling power exchange between electric utilities. Furthermore, load flow studies are necessary for performing a number of analyses, including state estimation, contingency planning, transient stability analysis, and voltage stability analysis. As a result, the primary computational tool for figuring out the operating conditions of the power system is load flow analysis. The active and reactive power injection at each bus, the phase angle and voltage magnitude at each bus, and the active and reactive power loss on each line are the main data gathered from the load flow analysis.

Two of these quantities are calculated, and two are stated for every bus. On the other hand, traditional techniques such as the rapid decoupling methods, modified Newton Raphson method, or Newton Raphson method are not appropriate for distribution systems. Because of their poorly conditioned meshed structure, these approaches only converge in transmission systems with large X/R ratios; in distribution networks, they are ineffective. Because of this, it is essential to analyze distribution networks using an effective load flow method(Philosophy, 2021).

2.7 Backward Forward Sweep load flow analysis

Compared to the traditional method, OPF performed using the BFS method uses less memory. The calculating procedure is quick and easy to use. The process consists of two consecutive sweeps: the forward sweep and the backward sweep, which compute the current values and adjust the corresponding voltages. The sequential numbering of branches is not necessary, in contrast to the traditional approach. To compute the current and power at each node, a branch identification system is instead used to assess the number of linked branches and connected nodes beyond a branch. The computation of every conceivable path is made possible by this technique (Shrivastava et al., 2015)(Ouali & Cherkaoui, 2020)(Jangid, 2017).

Forward sweep:

1. By using voltage drop computation to account for the currents or power flows fed into each lateral, the final voltages should be revised. The specified source voltage's boundary condition dictates this procedure.

2. With the possibility of updating current or power flow, the primary focus is on computing voltage decreases.

3. Update nodal voltages forward in a progressive manner, beginning with branches in the first layer and working your way up to the last layer.

4. At the feeder substation, the voltage is adjusted to reflect its actual value.

5. Keep the effective power in each branch constant at the value found by doing a backward traversal for the duration of the forward progression

Backward sweep:

1. Through current or power flow summing, the currents or power flows injected into each lateral are updated according on the end voltages. The boundary condition that there is no current or power flow out the end of the lateral applies to this update.

2. Beginning with the branches linked to the end node, the process moves forward to the branches linked to the source node.

3. During the backward propagation computation, the node voltages from the previous iteration are taken into consideration to update the effective power flows in each branch.

4. This indicates that while the updated power flows in each branch are transferred backward along the feeder using the backward path, the voltage values obtained in the forward path stay constant during the backward propagation.

2.8 Optimization Techniques

The optimal placement problem of various FACTS technologies has received a lot of attention lately, with various algorithms and goals being taken into account. One way to frame the FACTS device placement issue is as an optimization problem. Several algorithms are applied to the problem's solution. Three categories can be used to classify the approaches taken to overcome this issue (Chethan & Kuppan, 2024)(Prakash & Khatod, 2016).

- ❖ Analytical Methods
- ❖ Computational Methods
- ❖ Artificial Intelligence Methods

2.9 Flexible A.C. Transmission System (FACTS)

The core of FACTS was formulated over several decades, culminating in a novel idea that arose at the Electric Power Research Institute in the 1980s. High power electronic controllers are used in AC transmission networks by FACTS, or Flexible AC Transmission System. These controllers enable effective voltage and power flow regulation, guaranteeing dependable and quick operation. Instead of mentioning a single controller, FACTS refers to a group of controllers that system planners can select from using cost-benefit analysis.

A FACTS controller's primary goals are to control power flows in assigned transmission routes, guarantee safe line loading close to thermal limits, avoid cascading outages, dampen oscillations that could compromise line capacity or endanger security, and prevent voltage collapse by supporting reactive power. The active and reactive power flows in a transmission line can be precisely controlled by injecting a series voltage phasor with the desired magnitude and phase angle. This results in increased system stability, reliability, and lower operating and investment costs. Additionally, FACTS controllers play a crucial role in damping power system oscillations and compensating dynamic reactive power (Kaur & Gupta, 2021).FACTS device are categorized in different ways as shown figure 2.4.

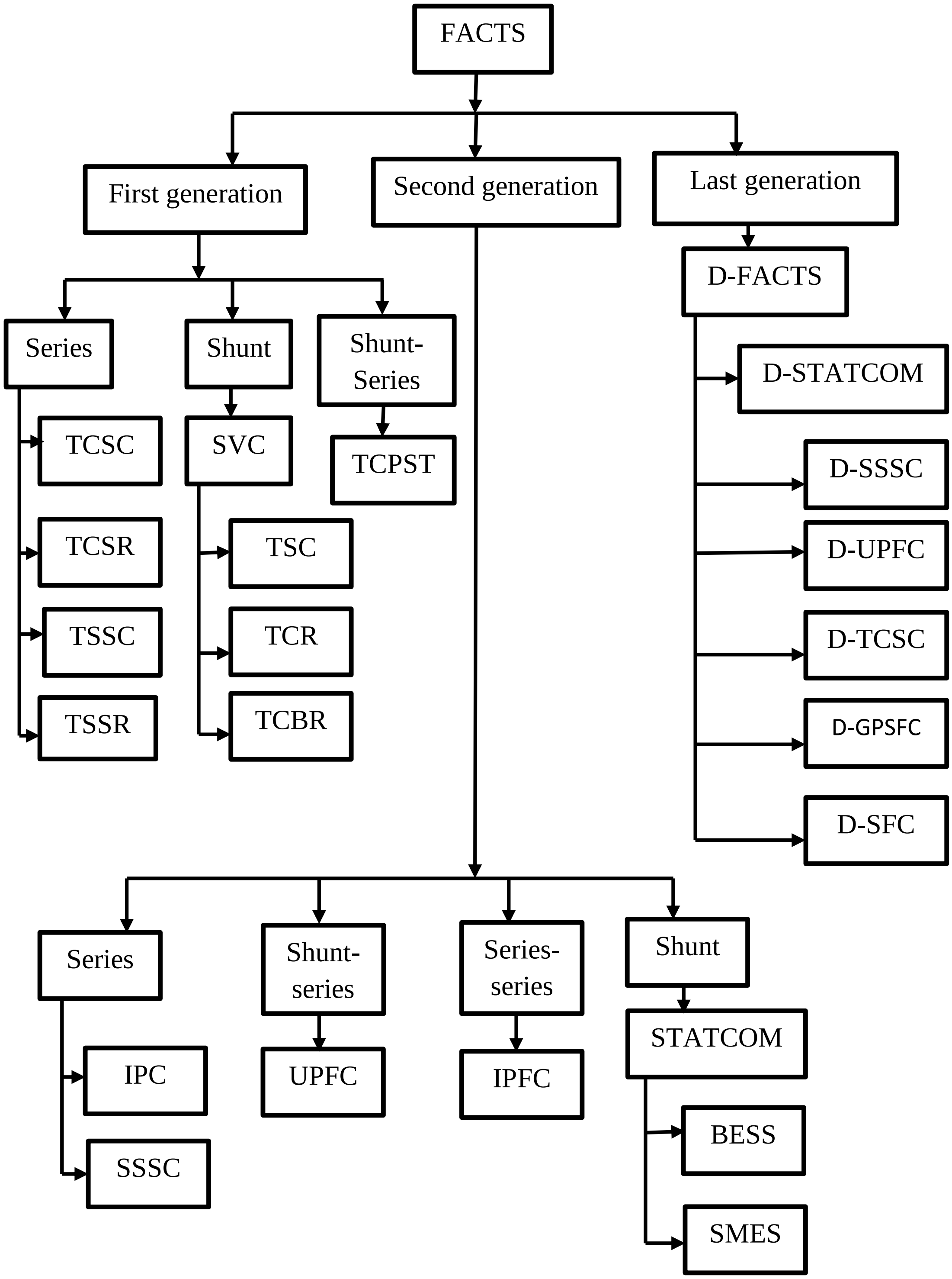

Figure 2.4 Classification of FACTS controllers (Albatsh et al., 2015)

Depending on how they are connected to the network, these controllers can be divided into four groups.

2.9.1 Shunt Controllers

SVC and STATCOM are examples of shunt FACTS controllers that are linked in parallel to the transmission line. They may have a variable source, variable impedance, or both. Injecting current into the system at the connection point is these controllers' primary job. The following are the main ways that SVC and STATCOM differ from one another: While STATCOM uses thyristor controlled reactors and thyristor switched capacitors to function as a shunt connected controlled reactive admittance, SVC uses a converter-based Var generation to work as a shunt connected synchronous voltage source.

As long as the reactive power injected by the shunt controller is in phase quadrature with the bus voltage, it can either inject or absorb reactive power into or out of the bus. Real power handling will be a part of any other phase relationship. If STATCOM has a DC terminal with an energy storage device, it can interchange actual power with the system (Jani & Makwana, 2018).

2.9.2 Series Controllers

TCSC, TCPAR, and SSSC are examples of series FACTS controllers that are connected in series with the transmission line. They can have a changing source of power electronics or switching impedance. Injecting electricity in series with the line is these controllers' main purpose. In the case of a switched impedance controller, the line's current flow plus the changing impedance combine to produce an injected voltage. As long as the current injected by the controller stays in phase quadrature with the bus voltage, the series controller can either inject or absorb reactive power. Real power management will also be a part of every other phase relationship (Manoj et al., 2017).

2.9.3 Combined Series-Series Controller

These controllers deal with the problem of compensating several transmission lines at a certain substation. The Interline Power Flow Controller (IPFC) is one of the most notable of them. Using the shared DC link, the IPFC can transfer actual power directly between the transmission lines. It also permits separate reactive series compensation control for every single line. The equalization of actual and reactive power flow between the lines is made possible by this special capacity. It also adjusts for resistive line voltage drops, fulfills the corresponding reactive power demand, and makes it easier for power to be transferred from overloaded to under loaded lines. In the end, the IPFC improves the entire compensatory system's efficacy, especially in the event of dynamic disturbances (Vairagade, 2017).

2.9.4 Combined Series-Shunt Controller

This gadget integrates independent shunt and series controllers that are controlled in a unified or coordinated way. Among the FACTS device family, the Unified Power Flow Controller (UPFC) is the most potent and adaptable. The UPFC can operate as a voltage regulator, phase shifter, power flow controller, shunt and/or series compensator, or as a voltage regulator depending on its primary control method. This makes it possible to adjust transmission line power flow and bus voltage simultaneously. Furthermore, if the UPFC's series and shunt components are united, real power can be transferred between a bus and a transmission line via the shared DC link (Narain, 2015).

2.10 Static Var Compensator (SVC)

The Static Var Compensator (SVC) is a shunt connected Var generator or absorber whose output is calibrated to exchange inductive or capacitive current in order to regulate or maintain particular electric power system parameters, most commonly bus voltage. It comes with different equipment for leading and lagging. Figure 2.5 shown below is a basic schematic of the SVC connection diagram.

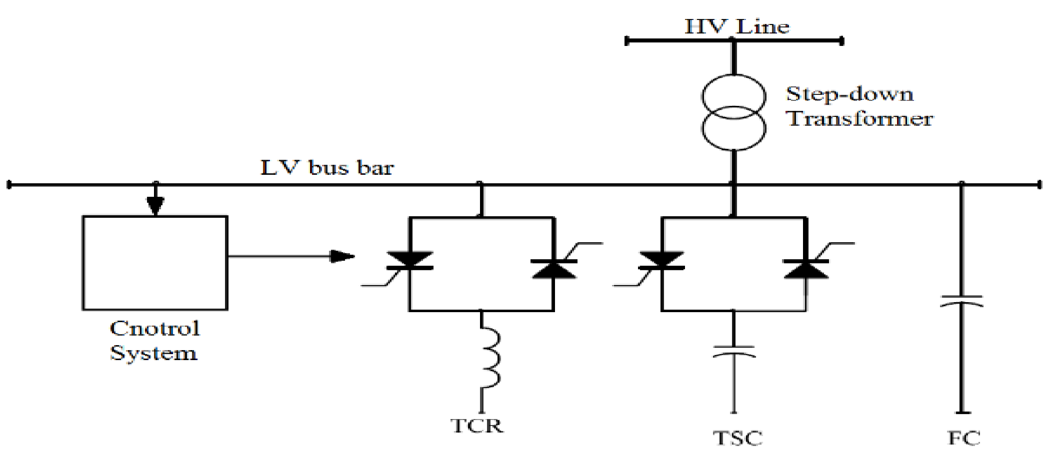

Figure 2.5 Configuration of a static var compensator(Khalil et al., 2021)

2.10.1 SVC Operating Principles

Maintaining the desired voltage at a high voltage bus is the control goal of SVC. In order to keep the voltage at the highest voltage bus at the predetermined level, the SVC will provide some steady-state voltage management. The SVC will inject reactive power (Q_{net}) into the system (within its control limits) if the voltage bus starts to drop below its set point range. This will raise the bus voltage back to the appropriate voltage level.

The target bus voltage will be reached if the bus voltage rises because the SVC will inject less reactive power or the TCR will absorb more of it (within its control limitations). According to the picture below, $+Q_{cap}$is a fixed value, which means that the amounts of reactive power added to the system are constant. The amount$-Q_{ind}$of reactive power that the TCR absorbs determinesQ_{net} (Mahdad, 2019).Figure 2.6 below shows Schematic diagram of TSC_TCR connection.

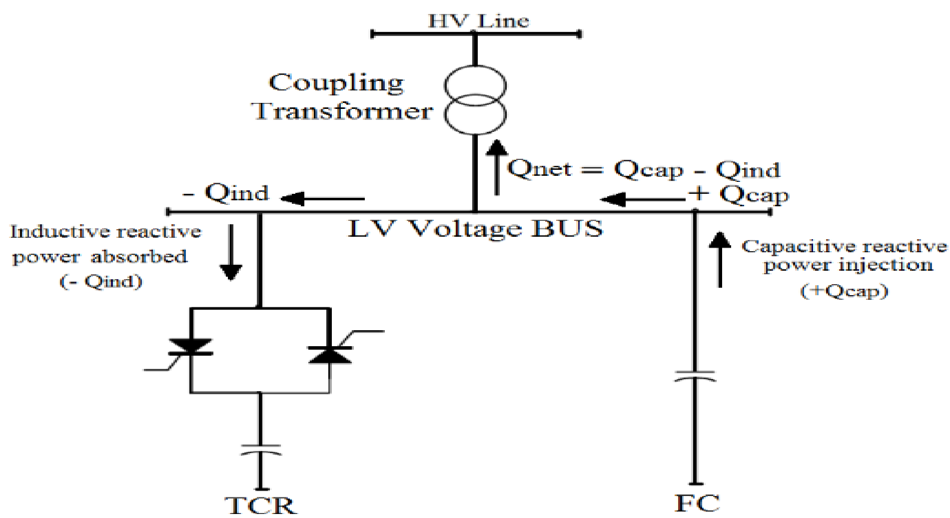

Figure 2.6 Schematic diagram of TSC_TCR (Chaurasiya et al., 2018)

2.10.2 Characteristics of SVC

Two modes of operation are available for the SVC: voltage regulation mode and var control mode (which maintains a constant SVC susceptance). The SVC implements the following V-I characteristic while it is in voltage regulation mode of operation. The voltage is regulated at the reference voltage V_{ref}as long as the SVC susceptance (B) remains within the maximum and lowest susceptance limits set by the total reactive power of the reactor banks(BL_{max}) and capacitor banks(BC_{max}).

Nonetheless, a voltage droop is typically employed (typically ranging from 1% to 4% at maximum reactive power production), and the slope of the V-I characteristic is depicted in the picture below (Turan et al., 2021). The following three equations describe the V-I characteristic. SVC is in regulation range ($-BC_{max} < B < BL_{max}$)

$$V=\frac{I}{BC_{max}} \quad (2.1)$$

$$V=V_{ref}+IX_s \quad (2.2)$$

Where SVC is fully capacitive (B=BC_{max})

$$V=\frac{I}{BL_{max}} \quad (2.3)$$

Where SVC is fully inductive (B=BL_{max})

Voltage – current characteristics of SVC is shown in figure 2.7 below.

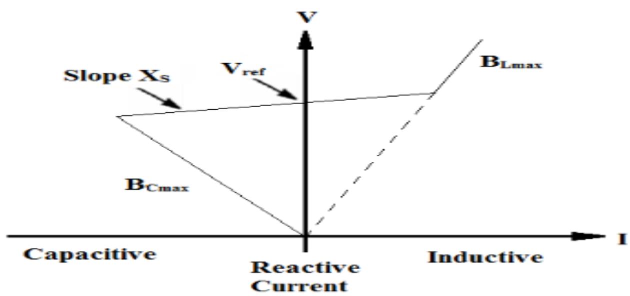

Figure 2.7 V-I Characteristics of SVC(Singh & Agrawal, 2018)

Currently in use, the following are the primary types of SVC controllers:

A. Thyristor Controlled Reactor (TCR)

Every phase of this specific Static Var Compensator setup includes a reactor with thyristor valves. By controlling the current passing through the reactor through the thyristor valves, reactive power can be adjusted. The ability of this kind of SVC to deliver smooth and continuous control sets it apart (Bimali & Pandey, 2022).

B. Fixed capacitor Thyristor Controlled Reactor (FC-TCR)

In this specific sort of SVC, a fixed capacitor bank and a TCR are used when reactive power generation is required. It is frequently regarded as the best choice for distribution and sub-transmission needs. This SVC variant's salient features include its compact construction, harmonics removal by fixed capacitor tuning, and smooth and continuous control (Terriche et al., 2021).

C.Thyristor Switched Capacitor (TSC)

This specific kind of Static Var Compensator (SVC) splits a bank of shunt capacitors into an appropriate number of branches. Anti-parallel linked thyristor independently activate or deactivate each branch. This SVC variant's salient characteristics include its minimal losses, adaptability, harmonic-free operation, and precise and seamless control (Dhivya, 2020).

D.Thyristor Controlled Reactor–Thyristor Switched Capacitor (TCR–TSC)

TCR and TSC together produce an ideal solution in many cases for this specific kind of SVC. The compensator's inductive and capacitive components can be fully controlled thanks to the TCR-TSC SVC's ability to generate continuously variable reactive power over the whole control range.

Its capacity to maintain peak performance in the face of severe system disruptions, such as line failures and load rejections, is its primary benefit. This kind of SVC is renowned for its low losses, redundancy, adaptability, continuous control, and harmonic removal via TSC control. But because these controllers are expensive, it is necessary to carefully consider where they should be placed in order to accomplish particular goals. SVC is frequently selected as the FACTS controller for improving voltage stability and lowering power losses due to its reduced cost (Taktode et al., 2019).

2.11 Related works

Different literature has proposed different techniques for the enhancement of distribution system performance. Such as FACTS device integration to the distribution lines with different methods. Much effort has been contributed to solving both optimal placement of SVC device the performance indices like power loss, voltage profile, and more are considered objective functions and the use of different techniques. The literature review includes some papers that take about SVC integration along with power flow analysis methods.

Table 2.1 below summarizes various studies on the Static Var Compensator (SVC), highlighting their objectives, methodologies, findings, and limitations, providing a clear comparison across different research efforts related to voltage stability in power systems.

Table 2.1 Related works comparisons

Author	Objective	Methodology	Findings	Gaps
Khalil et al. (2021)	Demonstrate the impact of SVC on voltage profiles in distribution systems.	Case study of a 33 KV distribution network in Tiwi city, Oman using ETAP software.	SVC installation reduced voltage drop from 6.2% to 3.39% and mitigated system power losses from 0.346 MW.	Suboptimal placement of SVC cannot increase performance of distribution system

Adebisi et al. (2017)	Enhance voltage stability and reduce power loss using SVC in IEEE bus networks.	Simulations of IEEE 6, 14, and 30-bus networks with and without SVC using MATLAB/PSAT.	Power losses decreased by 10.15%, 5.20%, and 1.06% for respective networks with SVC installed.	Lacks rationale for candidate bus selection and size of SVC
Access (2022)	Assess the impact of SVC on voltage stability through reactive power compensation.	Case study on Otowvodo 15MVA, 33/11kV substation using ETAP software.	Voltage at weak buses improved; identified buses for compensation based on load flow studies.	Does not analyze installation costs of SVCs.
Reports (2018)	Evaluate SVC technology for reducing fluctuations and enhancing voltage profiles.	Testing on IEEE-9 and IEEE-30 bus systems; optimization of placement and size of SVCs.	Improved voltage profiles and minimized losses; visual comparisons made with and without SVCs.	Newton-Raphson not applicable for distribution networks.
Gadal et al. (2023)	Overview of techniques to enhance voltage stability using various devices including SVCs.	Categorization of voltage stability indices and comparison analysis of FACTS devices in literature.	Provides guidelines for selecting appropriate VSIs; highlights contributions to voltage stability across configurations.	Voltage stability index lacks capability for multiobjective optimization problems.

CHAPTER THREE

3.SYSTEM DESCRIPTIONS AND METHODOLOGY

3.1Introduction

The materials and procedures employed, the case study area's history, the data that must be gathered, and the data analysis technique for gauging the performance of the current distribution system are all included in this chapter. Forward/Backward load flow analysis for power loss and voltage profile evaluation are the fundamental analyses used to assess the performance of the current radial distribution system. The modeling of SVC, its integration into the forward and backward sweep load flow, and the formulation of an optimization problem with its objective function and various constraints are all covered in this chapter. In conclusion, the application of particle swarm optimization (PSO) to resolve the pre-existing optimization problem pertaining to the ideal placement and size of SVC is examined.

3.2 Materials

In this thesis study, software such as Microsoft Office 2019, MathType6.0, MATLAB/2018a, Mendeley reference management, QGIS (Quantum Geographic Information System) and Visio are used. MATLAB/2018a is a software used for Particle Swarm Optimization algorithm code writing. Microsoft office is utilized for thesis document preparation and editing. Mathematical equations are written in Math Type 6.0. For citation, Mendeley Reference Manager is employed. The size of the distribution transformer and the separation between neighboring nodes are obtained using QGIS in order to obtain line data (resistance and reactance). Visio is an extremely potent drawing tool that may be used to draw a single line diagram of the outgoing feeder.

3.3 Methods

As seen in figure 3.1 below, several techniques and procedures are employed to complete the thesis work. It includes all required actions, beginning with the review of the relevant literature up to the conclusion of the thesis document.

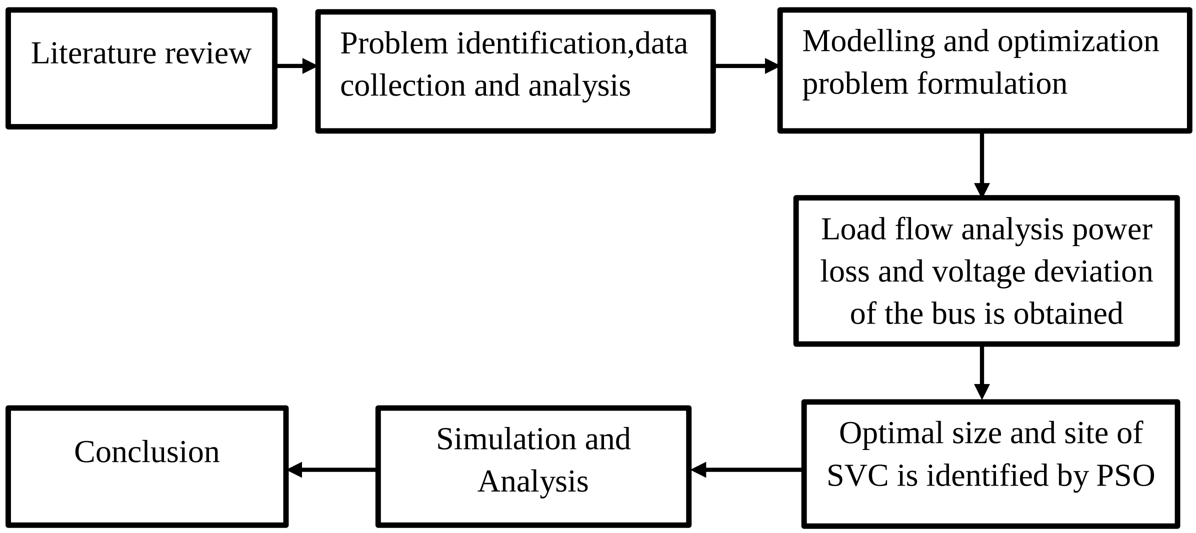

Figure 3.1 System Methodology flow diagram

First, a large number of publications pertaining to voltage profile enhancement and power loss mitigation are studied. Furthermore, a number of methods used to reduce power loss and voltage deviation in the radial distribution network are investigated.

Second, the relevant data are collected from Ethiopia Electric Utility and Ethiopia Electric Power (Gefersa Substation) and analyzed in accordance with established protocols. Line data, load data, pick load, and interruption data from the distribution network are all included in these data. Physical inspection of the substation and distribution system, interviews with substation workers, and review of the recorded data are the methods used to gather the data.

Thirdly, there is an archive of the mathematical models for Backward/Forward sweep, Static Var compensator, and Particle Swarm Optimization. Using a matlab code, the chosen feeder's backward and forward load flow analysis is completed, yielding the voltage and power loss profiles for all node. PSO determines the appropriate lacation and size of the SVC based on the acquired result.

Finally, load flow analysis is done a second time after the obtained size of SVC is placed on the appropriate bus. A conclusion is then made in light of the outcome that was attained.

3.4 Background of Case Study Area

The study is conducted in Gefersa Distribution Network, found in Burayu,sub-city Oromia region. Burayu is strategically located 15kmNorth from Addis Ababa. The town is located in the Shagar City, Oromia and has a Longitude and Latitude of 9°02′07″N 38°39′39″E .Gefersa Substation supply electric power to the Burayu city and the nearby areas and it receives power via two 132KV power lines from Holota Substation. Gefersa substation has sixty feeders,with ten 15kv feeder, five 33kv and one 45 kv.Geographical location of Gefersa substation is shown in figure 3.2 below.

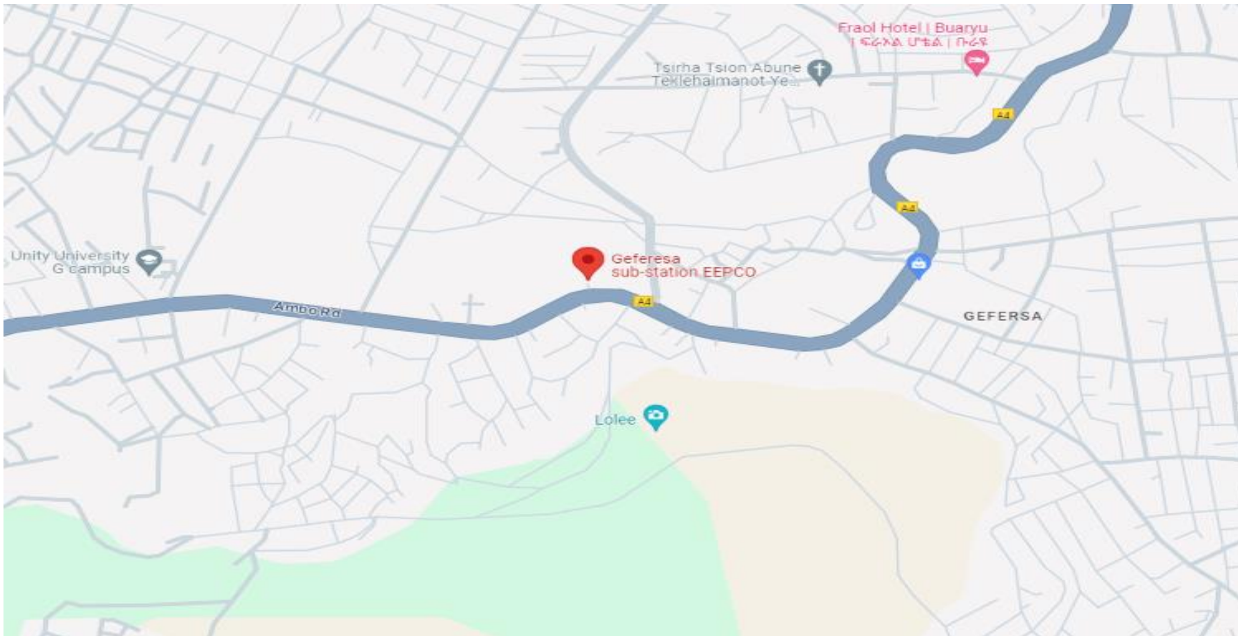

Figure 3.2 Location of Gefersa Distribution Substation

3.5 Single Line Diagram of the Selected Feeder

This thesis work focuses only on the primary distribution system of the Gefersa distribution system, which is 15kv voltage level. It includes from the substation to the distribution transformer which locates the different places in the city. The distribution line has three phases three-wire with a wooden pole and concrete along with radial configuration. Feeder 14 of the Gefersa outgoing is selected which has radial configuration. The feeder has 103 buses, 102 branches, eighty-eight distribution transformers, and fifteen common tapping nodes and it is constructed from the aluminum conductor (AAC-50mm^2 and AAC-95mm^2) with a total length of 31Km. All arrows in figure3.3indicate the load for each distribution transformer. The single line diagram of the outgoing line is drawn by concept Visio software as shown in figure 3.3. The line and load data of this feeder is found in Appendix-D

Gefersa 14 distribution feeder is selected based on:

- Permanent Fault occurred in the feeder
- Temporary Fault occurred in the feeder
- Peak Load (MVA and length of the feeder

Figure 3.3 Single line diagram of Line 14 feeder

3.6 Mathematical Model of for Radial Distribution Network

Assuming radial distribution networks are balanced and can also be represented by their equivalent single line diagram, we can examine a branch connecting buses m and n as shown below. In this case, the half-line charging susceptibility of the distribution lines is negligible, and they are depicted as short lines as shown in figure 3.4.

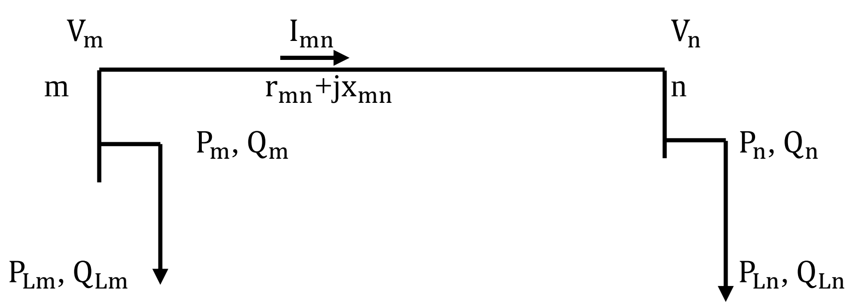

Figure 3.4 Single line diagram of distribution network with two nodes (Hamour et al., 2019)

The effective active (P_m) and reactive (Q_m) powers that of flowing through branch 'mn' from node 'm' to node 'n' can be calculated backwards from the last node is expressed as below.

The formula for calculating P_i and Q_i flowing through branch 'm' from node 'm' to node 'n' can be derived as follows:

$$P_m = P_n + P_{Ln} + \frac{V_m{}^2 - V_n{}^2}{r} \tag{3.1}$$

$$Q_m = Q_n + Q_{Ln} + \frac{V_m{}^2 - V_n{}^2}{x} \tag{3.2}$$

Where $P_m$effective active is power and Q_n is effective reactive power.

P_{Ln} and Q_{Ln} represent the loads connected at node 'n', and P_n and $Q_n$are the effective real and reactive power flows at node 'n'. The voltage magnitude at node 'm' is denoted by V_m, and at node 'n' by V_n. The impedance of branch 'mn' is represented by:

$$Z_{mn} = r_{mn} + jx_{mn} \tag{3.3}$$

Perhaps the voltage at node m denoted by $V_m\angle\delta_m$ and the voltage at node n denoted by $V_n \angle\delta_n$. Then the current flowing through branch 'mn' between node 'm' and n is given by:

$$I_{mn} = \frac{(V_m\angle\delta_m - V_n\angle\delta_n)}{Z_{mn}} \tag{3.4}$$

And it clear that the current through branch 'mn' can be given by

$$I_{mn} = \frac{(P_m - j\,Q_m)}{V_m\angle-\delta_m} \tag{3.5}$$

By equating equation (3.4) and (3.5)

$$\frac{(V_m\angle\delta_m - V_n\angle\delta_n)}{Z_m n} = \frac{(P_m - j\,Q_m)}{V_m\angle-\delta_m} \tag{3.6}$$

$$(r_{mn} + jx_{mn}) * (P_m - j\,Q_m) = (V_m\angle\delta_m - V_n\angle\delta_n) * V_m\angle-\delta_m \tag{3.7}$$

$$r_{mn}\,P_m + jx_{mn}P_m - jQ_m r_{mn} + x_{mn}Q_m = V_m{}^2 - V_mV_n\angle(\delta_n - \delta_m) \tag{3.8}$$

$$V_m{}^2 - P_m r_{mn} + Q_m x_{mn} - V_mV_n\cos(\delta_n - \delta_m) - j\,(P_m x_{mn} + Q_m r_{mn}) + j\,V_mV_n\sin(\delta_n - \delta_m) = 0 \tag{3.9}$$

After equating imaginary and real parts on both side

$$V_m{}^2 - P_m r_{mn} + Q_m x_{mn} - V_mV_n\cos(\delta_n - \delta_{mn}) = 0 \tag{3.10}$$

$$j(\,P_m x_{mn} + Q_m r_{mn}) + j\,V_mV_n\sin(\delta_n - \delta_{mn} = 0 \tag{3.11}$$

Squaring and adding equation (3.10) and (3.11)

$$(V_mV_n)^2 - [V_m{}^2 - (P_m r_{mn} + Q_m x_{mn})^2]^2 - (Q_m r_{mn} - P_m x_{mn})^2 = 0 \tag{3.12}$$

And from trigonometric formula, $\cos(\delta_t)^2 + \cos(\delta_t)^2 = 1$. Where $\delta_t = \delta_n - \delta_m$

$$(V_mV_n)^2 - V_m{}^4 + 2V_m{}^2(P_m r_{mn} + Q_m x_{mn})^2 - [P_m{}^2 + Q_m{}^2] * [r_{mn}{}^2 + x_{mn}{}^2] = 0 \tag{3.13}$$

Solving for V_n

$$V_n{}^2 = \frac{V_m{}^4 - 2V_m{}^2(P_m r_{mn} + Q_m x_{mn})^2 + [P_m{}^2 + Q_m{}^2] * [r_{mn}{}^2 + x_{mn}{}^2]}{V_i{}^2} \tag{3.14}$$

$$V_n{}^2 = V_m{}^2 - 2(P_m r_{mn} + Q_m x_{mn})^2 + [r_{mn}{}^2 + x_{mn}{}^2]\frac{[P_m{}^2 + Q_m{}^2]}{V_m{}^2} \tag{3.15}$$

$$\delta_n = (\delta_m) + \tan^{-1}\frac{[Q_m x_{mn} - P_m r_{mn}]}{[V_m{}^2 - (r_{mn} + Q_m x_{mn})]} \tag{3.16}$$

$$P_{loss}(mn) = r_{mn}\frac{[Q_m{}^2 + P_m{}^2]}{V_m{}^2} \tag{3.17}$$

where $P_{loss}(mm)$ is the active power loss through the branch 'mn'.

$$Q_{loss}(mn) = x_{mn}\frac{[Q_m{}^2 + P_m{}^2]}{V_m{}^2} \tag{3.18}$$

where $Q_{loss}(mn)$ is the reactive power loss through the branch 'mn'.

For the radial distribution system, the total active power loss of branch 'mn' ($PL_{total}(mn)$ and the total reactive power loss of branch 'mn' is calculated as follows.

$$PL_{total}(mn) = \sum_{mn=1}^{k} r_{mn}\frac{[Q_m{}^2 + P_m{}^2]}{V_m{}^2} \tag{3.19}$$

where k is number of branch

$$QL_{total}(mn) = \sum_{mn=1}^{k} x_{mn}\frac{[Q_m{}^2 + P_m{}^2]}{V_m{}^2} \tag{3.20}$$

Initially, a flat voltage profile is assumed at all nodes i.e., 1.0 pu. The branch powers are computed iteratively with the updated voltages at each node. In the proposed load flow method, powers summation is done in the backward ward and voltages are calculated in the forward ward.

3.7 Mathematical Model of Backward/Forward Sweep method

On Kirchhoff's current law and voltage laws, the Backward/Forward sweep load flow analysis is based. There are two steps in the BFS process: the forward sweep and the backward sweep (Salimon et al., 2019).

Backward Sweep: The following formula can be used to determine the load current of each bus in a radial distribution network with n nodes once the load data for the network has been obtained.

$$\overline{I_L}(i) = \frac{P_{L(i)} - jQ_{L(i)}}{\overline{V^*}(i)} \qquad i=1, 2, 3\ldots\ldots n \tag{3.21}$$

Where $P_{L(i)}$ and$Q_{L(i)}$ represents the real and reactive loads at node 'i' and over bar indicates the phasor quantities. The branch current of the network is calculated by:

$\bar{I}$ (ij)= $\bar{I_L}$(n) +Summation of all node current beyond node n

Forward Sweep: The distribution network's node voltage in a forward sweep is computed as follows:

$$\bar{V}(j)= \bar{V}(i) - \bar{I}(ij)\, Z(ij) \tag{3.22}$$

Where i and j represents two adjacent nodes connected by branch ij and Z (ij) is the impedance of the branch.

The Forward-Backward sweep is predicated on the node injection to branch current matrix (BIBC), branch current to node voltage matrix (BCBV), and Equivalent Current Injection (ECI).

Calculation of node (load current) current:

The more popular mathematical model for radial distribution networks uses current injection. The apparent power S_i for any given node or bus can be computed using the following formula:

$$S_i=P_i+Q_i \qquad i=1, 2, 3, 4, 5\ldots.n \tag{3.23}$$

And the node current at k^{th} iteration is given by

$$I_i^k = \left(\frac{P_i + jQ_i}{V_i^k}\right)^* \tag{3.24}$$

Where V_i^k and I_i^k are the node voltage and current of node (bus) i at the k^{th} iteration respectively.

3.7.1BIBC Matrix Formulation

The relationship between the branch and bus current injections can be found by applying KCL to the distribution system. As a function of current injections, the branch currents are shown. For example, branch currents I_{b1},I_{b2}, I_{b3},I_{b4}, I_{b5}can be expressed as in figure 3.5.

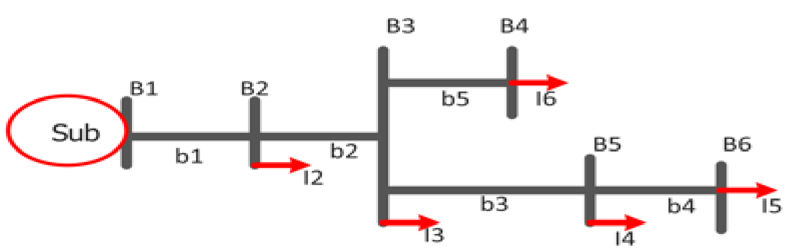

Figure 3.5 Distribution network with six nodes(Salimon et al., 2019)

$$I_{b1}=I_2+I_3+I_4+I_5+I_6$$

$$I_{b2}=I_3+I_4+I_5+I_6 \tag{3.25}$$

$I_{b3}=I_4+I_5$

$I_{b4}=I_5$

$I_{b5}=I_6$

The relationship between the branch and bus current injections can be expressed as

$$\begin{pmatrix} I_{b1} \\ I_{b2} \\ I_{b3} \\ I_{b4} \\ I_{b5} \end{pmatrix} = \begin{pmatrix} 11111 \\ 01111 \\ 00110 \\ 00010 \\ 00001 \end{pmatrix} * \begin{pmatrix} I_2 \\ I_3 \\ I_4 \\ I_5 \\ I_6 \end{pmatrix} \quad (3.26)$$

Therefore, equation (3.26) be expressed as

$$[I_b]=[BIBC][I_n] \quad (3.27)$$

where the bus injection to branch current matrix is represented by BIBC.

3.7.2 Algorithm for the Development of BIBC Matrix

The BIBC matrix algorithm can be developed as follows using the equations above:

Step1: In the case of a radial distribution system with n buses and m branches, the BIBC matrix dimension is mx(n-1).

Step 2: In case a branch (B_k) is situated between the i and j buses, transfer the i^{th}bus column to the j^{th}bus column and indicate +1 at the k^{th}row and j^{th} column positions.

Step3: Repeat step 2 until all branch sections are represented in the BIBC.

3.7.3 BCBV Matrix Formulation

This step involves the calculation of each bus voltage using the Kirchhoff Voltage Laws (KVL), taking into account the impedance of each line as well as the branch current that was determined in the first stage, working from the source node to the end node. Finally, the following formula is used to create the Branch-Current to Bus Voltage (BCBV) matrix and the bus voltage from V_2 to V_6 were expressed as follows.

$$V_2 = V_1 - Ib_1Z_{12}$$
$$V_3 = V_2 - Ib_2Z_{23} = V_1 - Ib_1Z_{12} - Ib_2Z_{23}$$
$$V_4 = V_3 - Ib_3Z_{34} = V_1 - Ib_1Z_{12} - Ib_2Z_{23} - Ib_3Z_{34} \quad (3.28)$$
$$V_5 = V_4 - Ib_4Z_{45} = V_1 - Ib_1Z_{12} - Ib_2Z_{23} - Ib_3Z_{34} - Ib_4Z_{45}$$

$$V_6=V_5-Ib_5Z_{56}=V_1 - Ib_1Z_{12} - Ib_2Z_{23} - Ib_3Z_{34} - Ib_4Z_{45} - Ib_5Z_{56}$$

Therefore, the relationship between branch currents and bus voltages can be expressed as:

$$\begin{bmatrix} V_1 \\ V_1 \\ V_1 \\ V_1 \\ V_1 \end{bmatrix} - \begin{bmatrix} V_2 \\ V_3 \\ V_4 \\ V_5 \\ V_6 \end{bmatrix} = \begin{bmatrix} Z_{12} & 0 & 0 & 0 & 0 \\ Z_{12} & Z_{23} & 0 & 0 & 0 \\ Z_{12} & Z_{23} & Z_{34} & 0 & 0 \\ Z_{12} & Z_{23} & Z_{34} & Z_{45} & 0 \\ Z_{12} & Z_{23} & 0 & 0 & Z_{56} \end{bmatrix} \begin{bmatrix} Ib_1 \\ Ib_2 \\ Ib_3 \\ Ib_4 \\ Ib_5 \end{bmatrix} \quad (3.29)$$

The general form of equation (3.29) is expressed as

$$\Delta V=[BCBV][I_b] \quad (3.30)$$

For the given sample network BCBV matrix is expressed as:

$$[BCBV]=\begin{bmatrix} 1 & 0 & 0 & 0 & 0 \\ 1 & 1 & 0 & 0 & 0 \\ 1 & 1 & 1 & 0 & 0 \\ 1 & 1 & 1 & 1 & 0 \\ 1 & 1 & 0 & 0 & 1 \end{bmatrix} \begin{bmatrix} Z_{12} & 0 & 0 & 0 & 0 \\ 0 & Z_{23} & 0 & 0 & 0 \\ 0 & 0 & Z_{34} & 0 & 0 \\ 0 & 0 & 0 & Z_{45} & 0 \\ 0 & 0 & 0 & 0 & Z_{56} \end{bmatrix} \quad (3.31)$$

$$[BCBV]=\begin{bmatrix} 1 & 1 & 1 & 1 & 1 \\ 0 & 1 & 1 & 1 & 1 \\ 0 & 0 & 1 & 1 & 0 \\ 0 & 0 & 1 & 1 & 0 \\ 0 & 0 & 0 & 0 & 1 \end{bmatrix}^T \begin{bmatrix} Z_{12} & 0 & 0 & 0 & 0 \\ 0 & Z_{23} & 0 & 0 & 0 \\ 0 & 0 & Z_{34} & 0 & 0 \\ 0 & 0 & 0 & Z_{45} & 0 \\ 0 & 0 & 0 & 0 & Z_{56} \end{bmatrix} \quad (3.32)$$

The general form of equation (3.32) can be expressed as:

$$[BCBV]=[BIBC]^T[Z_D] \quad (3.33)$$

$$\begin{bmatrix} V_1 \\ V_1 \\ V_1 \\ V_1 \\ V_1 \end{bmatrix} - \begin{bmatrix} V_2 \\ V_3 \\ V_4 \\ V_5 \\ V_6 \end{bmatrix} = \begin{matrix} 1 & 0 & 0 & 0 & 0 \\ 1 & 1 & 0 & 0 & 0 \\ 1 & 1 & 1 & 0 & 0 \\ 1 & 1 & 1 & 1 & 0 \\ 1 & 1 & 0 & 0 & 1 \end{matrix} \begin{bmatrix} Z_{12} & 0 & 0 & 0 & 0 \\ 0 & Z_{23} & 0 & 0 & 0 \\ 0 & 0 & Z_{34} & 0 & 0 \\ 0 & 0 & 0 & Z_{45} & 0 \\ 0 & 0 & 0 & 0 & Z_{56} \end{bmatrix} \begin{bmatrix} Ib_1 \\ Ib_2 \\ Ib_3 \\ Ib_4 \\ Ib_5 \end{bmatrix} \quad (3.34)$$

The general form of equation (3.34) can be expressed as:

$$[\Delta V]=[BIBC]^T[Z_D][I_b] \quad (3.35)$$

Putting equation (3.27) in to (3.30), we obtain

$$[\Delta V] = [BCBV][BIBC][I_n] \quad (3.36)$$

Putting equation (3.33) in to (3.36), we obtain

$$[\Delta V]=[BIBC]^T[Z_D][BIBC][I_n] \quad (3.37)$$

The distribution load flow matrix is formulated as:

$$[DLF]=[BCBV][BIBC] \quad (3.38)$$

Putting equation (3.33) in to (3.38), we obtain

$$[DLF]=[BIBC]^T[Z_D][BIBC] \quad (3.39)$$

Therefore, equation (3.37) can be expressed as:

$$[\Delta V]=[DLF][I_n] \quad (3.40)$$

$$I_i^k = \left(\frac{P_i + jQ_i}{V_i^k}\right)^* \quad (3.41)$$

$$[\Delta V^{K+1}]=[DLF][I_n^k] \quad (3.42)$$

$$V^{k+1} = [v^0] + [\triangle V^{k+1}] \quad (3.43)$$

In the first iteration, compute the load current under the initial assumption that all nodes have constant voltages. Additionally, the procedure is repeated utilizing the new voltages until the convergence conditions are met.

For thek^{th}iteration n^{th}node the convergence criteria is reached when

$e_{\max} = \max(V_n^{k+1} - V_n^k) \leq$ tolerance limit

3.7.4 Algorithm for the Development of BCBV Matrix

The BCBV matrix algorithm can be developed as follows using the equation above.

Step1: In the case of a radial distribution system with n buses and m branches, the BCBV matrix dimension is (n-1)xm

Step 2: In case a branch (B_k) is located between the i and j buses, transfer the row of the i^{th} bus to the j^{th} bus's column and indicate +1 at the k^{th} row and j^{th} column's position.

Step3: Repeat step 2 until all branch sections are represented in the BCBV.

3.5.5 Algorithm of Backward-Forward Sweep Power Flow Analysis

Step1: Read line data and load data of the radial distribution network.

Step2: Calculate the node current (bus current) using equation (3.41).

Step3: Form BIBC matrix using equation given in (3.26).

Step4: Calculate branch current using BIBC matrix and current injection matrix as given in equation (3.27).

Step5: Form the BCBV matrix using equation given in (3.33).

Step6: Calculate the DLF matrix by using equation given in (3.39).

Step7: Set iteration k=1

Step8: Iteration k=k+1

Step9: Update node voltages using equation given in (3.41), (3.42) and (3.43).

Step10:If $e_{\max} = \max(V_n^{k+1} - V_n^k) \leq$ tolerance limit print results else update iteration.

Flow chart of Backward/Forward load flow analysis is shown below in figure 3.6.

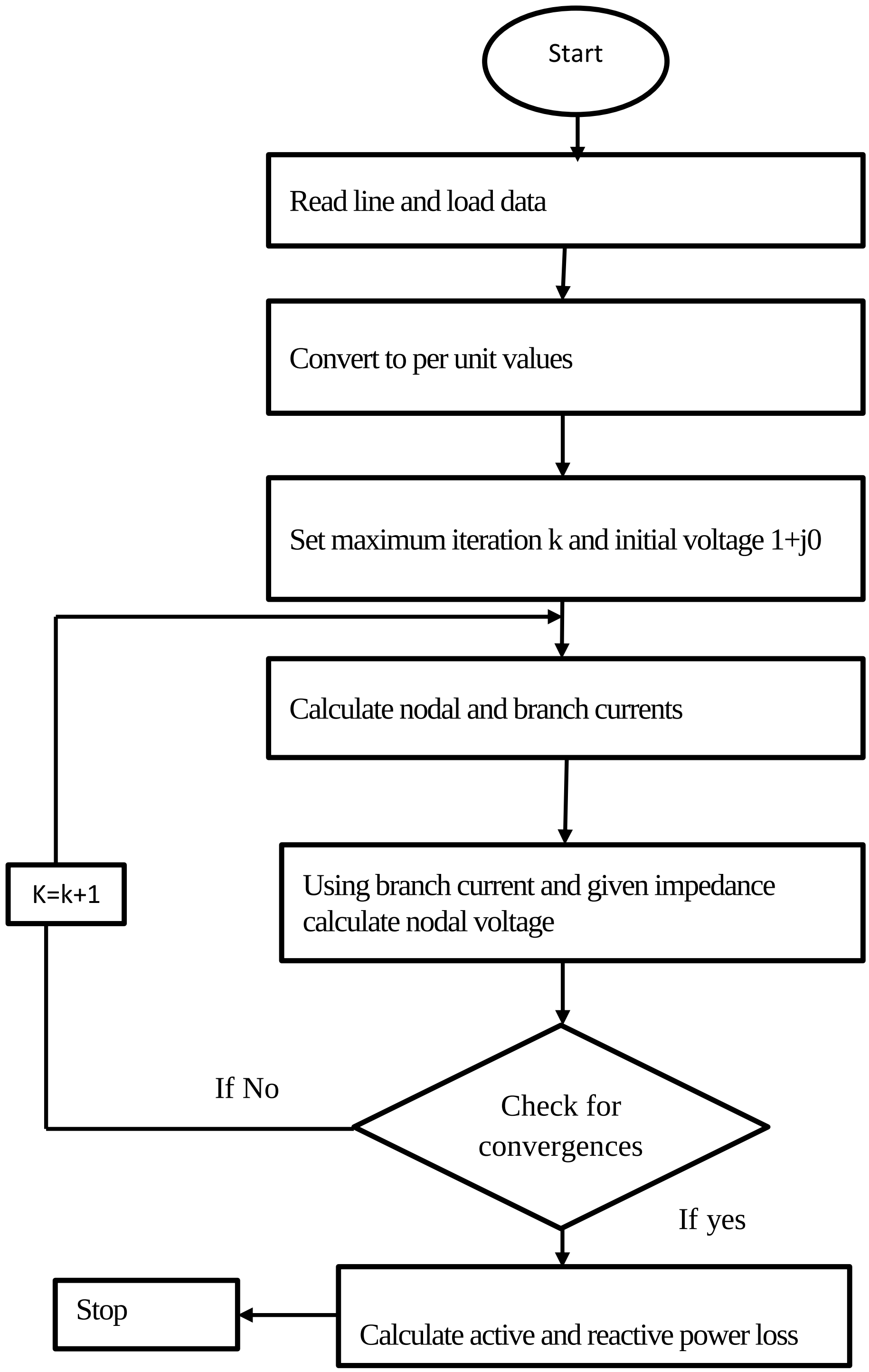

Figure 3.6 Flow chart of Backward/Forward load flow analysis

3.8 Per Unit Calculation in Power flow analysis

In power System, the per-unit system is a mathematical technique that expresses quantities in relation to a selected base value, thereby normalizing and simplifying electrical computations. When examining and contrasting electrical systems, apparatus, and parts, it is especially helpful. Expressing quantities in relation to a selected base value is known as normalization. Base values are predefined benchmarks that depict typical power system operating conditions.

$$\text{Per Unit Value}=(\text{Actual Value})/(\text{Base Value}) \tag{3.44}$$

MVA Base (S_{base}): MVA base represents the base apparent power for per unit calculations and is typically chosen based on the rating of a reference component in the system.

KV Base (KV_{base}): KV base represents the base voltage for per unit calculations and is typically chosen based on the rated voltage of the system.

Z Base (Z_{base}): Z base represents the base impedance for per unit calculations and is derived from the chosen MVA base and kV base.

$$Z_{base} = \frac{{KV_{base}}^2}{MVA_{base}} \tag{3.45}$$

R_{pu} (Per Unit Resistance): Per unit resistance (R_{pu}) is the ratio of the actual resistance (R) to the base impedance (Z_{base}).

$$R_{pu} = \frac{R_{actual}}{Z_{base}} \tag{3.46}$$

X_{pu} (Per Unit Reactance): Per unit reactance (x_{pu}) is the ratio of the actual reactance (X) to the base impedance (Z_{base}).

$$X_{pu} = \frac{X_{actual}}{Z_{base}} \tag{3.47}$$

P_{pu} (Per Unit Active Power):

Per unit active power (P_{pu}) is the ratio of the actual active power (P) to the MVA base (S_{base}).

$$P_{pu} = \frac{P_{actual}}{1000* MVA_{base}} \tag{3.48}$$

Q_{pu} **(**Per Unit Reactive Power):

Per unit reactive power (Q_{pu} =) is the ratio of the actual reactive power (Q) to the MVA base

$$(S_{base})Q_{pu} = \frac{Q_{actual}}{1000* MVA_{base}} \tag{3.49}$$

3.9 Modeling of Particle Swarm Optimization Algorithm

Kennedy and Eberhart used the behavior of a flock of birds to propose a solution to a complex, non-linear optimization issue. They created the idea of employing a swarm of particles to optimize the function. Consider a function of n dimension which is defined by:

$$f(x_1, x_2, x_3 \ldots\ldots x_n) = f(x) \quad (3.50)$$

Where x_i is the optimizing variable, which represents the set of variables for a given function $f(x)$. Here, the goal is to get an optimum value x* so that the function f(x*) can become either a maximum value or a minimum value.

Particle swarm optimization is a parallel search strategy that makes use of several agents. A solution is represented by each member in the swarm. Every agent explores the whole search space and modifies its position and velocity based on both their own and other agent's experiences. Suppose xi^t denote the agent or particle 'i' position vector search space at time step t, then each agent position is updated in the search space by:

$$xi^{t+1} = xi^t + vi^{t+1} \quad (3.51)$$

where, vi^t is the particle velocity vector which is used to update the own experience and other particles experience and also drives the optimization process. As a result, the PSO technique initializes each agent at random and computes the fitness value by updating the global best, which is the best value of all the agents in the swarm, as well as the personal best, which is the best value of each agent. The loop begins by taking the starting particle positions to be the individual best values, and it then uses the updated velocity to update each particle's position. The loop will terminate when the stopping condition is satisfied(Wang et al., 2017).Flow chart of particle swarm optimization is shown in figure 3.7.

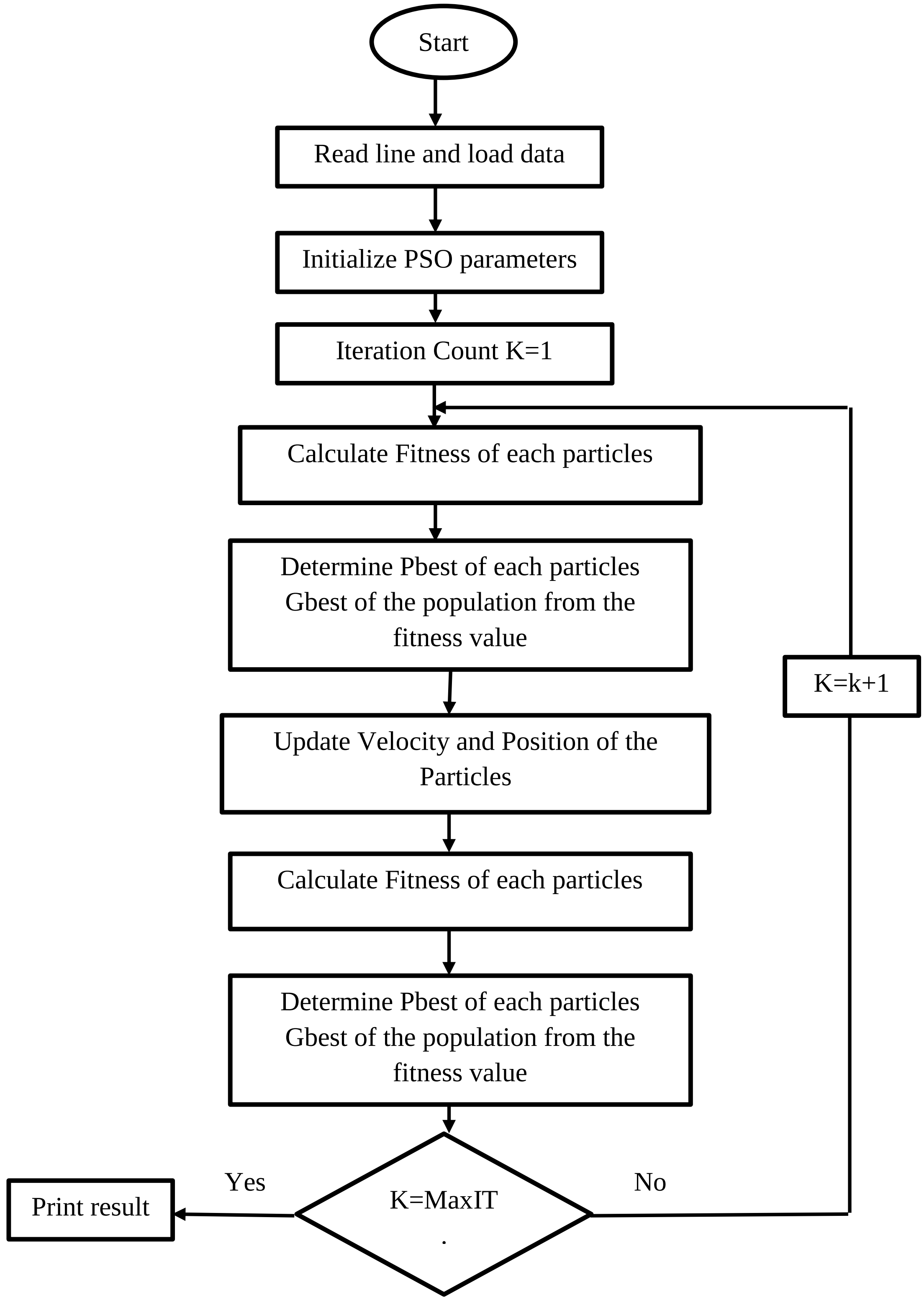

Figure 3.7 Flow Chart of PSO

3.9.1Global Best Particle Swarm Optimization

The global best position in Particle Swarm Optimization (PSO) is the location in the search space where all of the particles in the population have the best fitness value. It stands for the greatest outcome that any particle discovered during the whole optimization procedure. The local best position, or the place that each particle in the PSO algorithm has found so far with the best fitness value, is what it refers to as its local best position. The location with the best fitness value among all the particles, known as the global best position, is also maintained by the population as a whole.

The particles adjust their positions and velocities according to both the global and local optimal placements throughout each iteration of the PSO algorithm. The particles use the global best location as a guide to go across the search space and arrive at the best solution.

The global best position is typically determined by comparing the fitness values associated with each particle's current position. The quality or objective value of the solution is represented by the fitness value. As the global best position, the particle with the best fitness value contributes to it. This approach utilizes a star network topology in order to gather information from every member in the swarm.

PSO promotes cooperative behavior among the particles by allowing them to share knowledge about the global optimal position and work together to find better solutions. Throughout the optimization process, as particles scan the search space and maybe find superior solutions, the global best position is updated continuously. Ultimately, by directing the particles toward interesting areas of the search space and aiding in the hunt for the optimum solution, the global best position is vital to the PSO algorithm.

In this case, x_i represents each agent's current location in search space, $v_i$denotes their current velocity, and a Pbest,i is each agent's personal best position in search space. When a minimization problem is taken into account, the particle "i" position in the search space with the smallest fitness function value is represented by the personal best position Pbest, i. Gbest is the particle position that, when compared to all other personal best places, produces the lowest value (Shami et al., 2023). Flow chart of global best PSO is shown in figure 3.8.

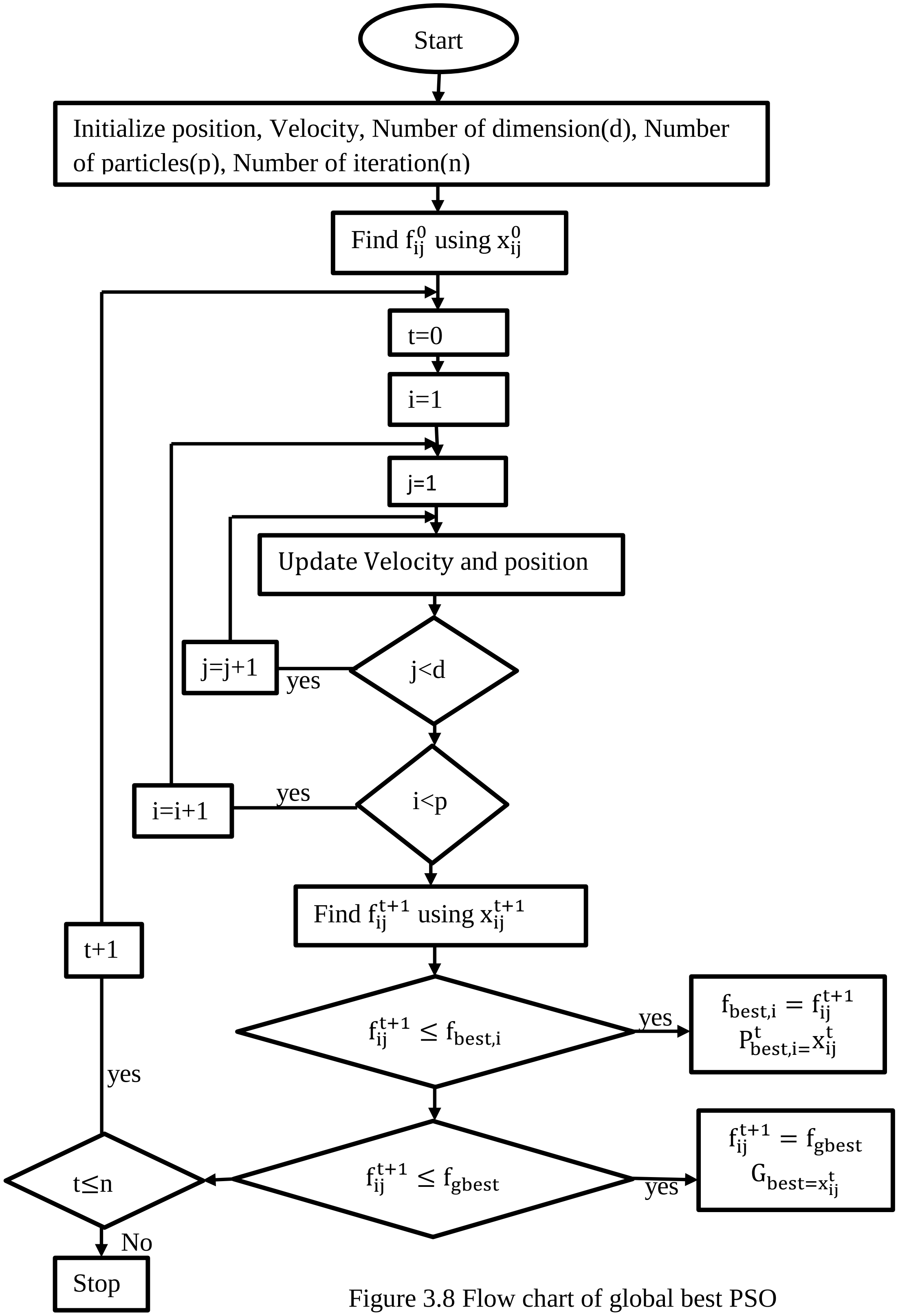

Figure 3.8 Flow chart of global best PSO

3.9.2 Local Best Particle Swarm Optimization

By using the Local Best PSO (lbest PSO) technique, a ring-like local social topology is created where each agent is impacted by the best agent among its neighbors. Local knowledge of the environment is represented in this manner by the social information that is shared among the agents in the area (Engelbrecht, 2016). The particle's velocity is calculated by:

$$V_{ij}^{t+1}=\omega V_{ij}^{t}+c_1 r_{1j}^{t}(P_{best,i}^{t}\_x_{ij}^{t})+ c_2 r_{2j}^{t}(L_{best,i}\_x_{ij}^{t}) \quad (3.54)$$

where, $L_{best,i}$ is the best position that a particle has had in the neighborhood of particle 'i 'obtained from initialization through time t.

Personal best (Pbest, i) for a minimization problem at step t+1, where tϵ[0…n], is computed as follows:

$$P^{t+1}{}_{best,i}=\begin{cases} P^{t}{}_{best,i} if, f(x_i^{t+1}) > P^{t}{}_{best,i} \\ x_i^{t+1} if, f(x_i^{t+1}) \leq P^{t}{}_{best,i} \end{cases} \quad (3.52)$$

For a minimization problem, the global best position(Gbest)at time step is computed as:

$G_{\mathrm{best}}=\min(\mathrm{P}_{\mathrm{best,i}}^{\mathrm{t}})$, Where $\mathrm{i} \in (1 \ldots \ldots \ldots .\mathrm{n})$and $\mathrm{n} > 1$

It may be observed that the optimal position of each agent over all time steps is their personal best. The best position of every agent in the entire swarm is referred to as global best.

For gbest PSO method, velocity of agent is obtained by:

$$V_{ij}^{t+1}=\omega V_{ij}^{t}+c_1 r_{1j}^{t}(P_{best,i}^{t}\_x_{ij}^{t})+ c_2 r_{2j}^{t}(G_{best}\_x_{ij}^{t}) \quad (3.53)$$

Where,

V_{ij}^{t} is Velocity of the particle in the swarm at time t

x_{ij}^{t} is position of particle in the swarm at time t

$P_{best,i}^{t}$ is Particle's personal best position within the swarm

G_{best} is Global best position of the particle in the swarm

c_1 and c_2 are acceleration constant

r_{1j}^{t} and r_{2j}^{t} are random number generated at time t

Flow chart of local best PSO is shown below in figure 3.9.

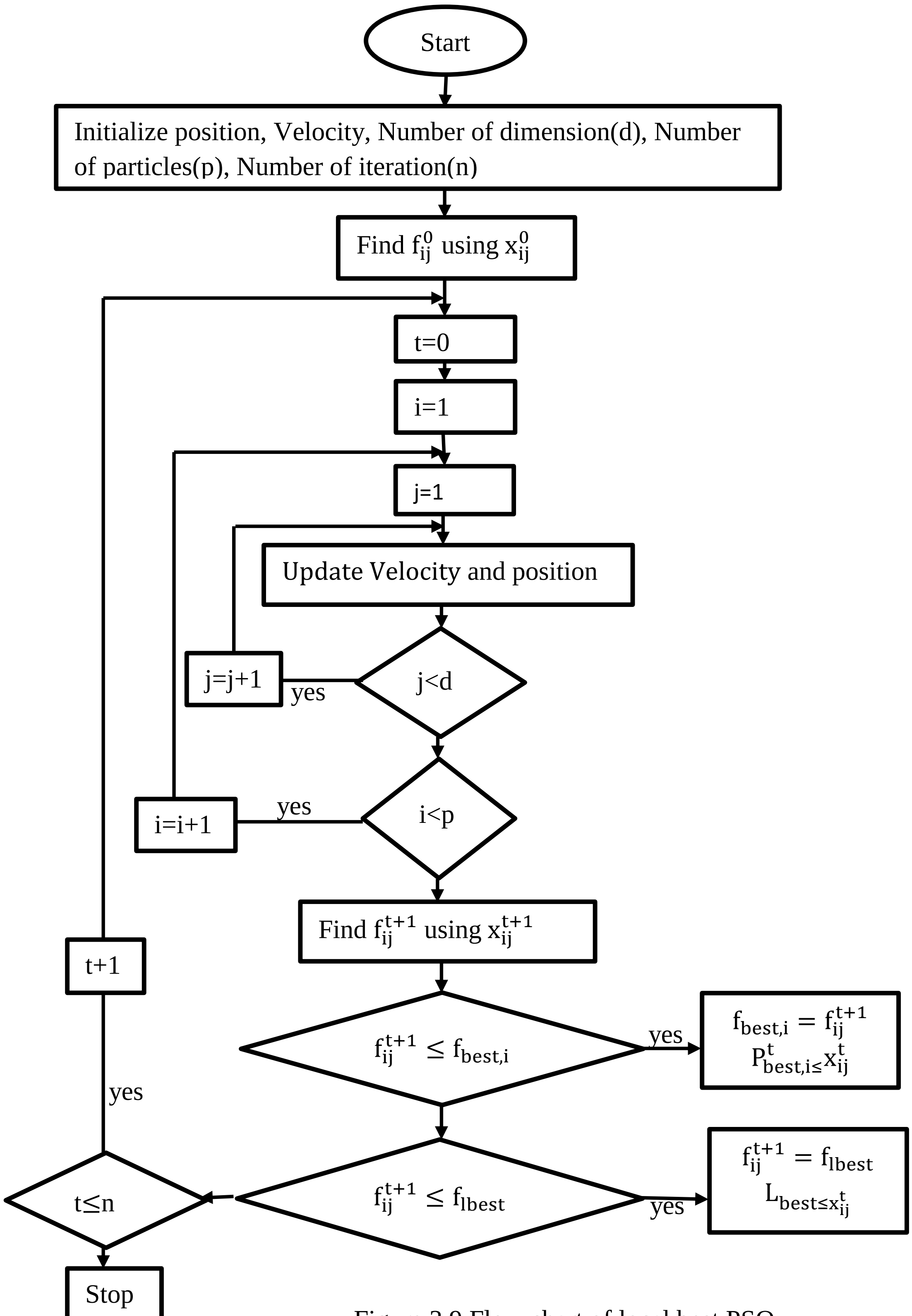

Figure 3.9 Flow chart of local best PSO

3.10 Particle Swarm Optimization Parameters

Certain settings in the Particle Swarm Optimization (PSO) algorithm can significantly affect its performance and efficiency, while other factors may have less of an impact. In PSO, selecting the right parameter values is essential to obtaining strong convergence and exploration capabilities. Some of the crucial PSO parameters and how they affect the algorithm's performance are as follows (Sakthivel et al., 2016).

a. Swarm Size

The number of agents or particles in the population is referred to as the swarm size in the PSO method. More particles participate in the search process and cover a greater area of the search space during each iteration when the swarm size is larger. On the other hand, the computational complexity and iteration time may rise with a large number of agents used. Based on prior research and actual findings, it is generally advised to select a swarm size between 20 and 60 in order to achieve a balance between exploration and processing efficiency. Numerous optimization issues have been discovered to benefit from this range(Piotrowski et al., 2020).

A particle is composed of three vectors

- The particle's current position in the search space is recorded by the x-vector, also known as the position vector.
- The location of the particle's current best solution, both local and global, is indicated by the p-vector(pbest).
- If particles are not disturbed, they proceed in a direction indicated by the gradient found in the v-vector, or velocity vector. With every iteration, three of them are updated.

b. Iteration Numbers

To achieve the optimal optimization outcome, the PSO algorithm's iteration count is a key factor. The particular problem being solved determines how many iterations are necessary. An excessively low number of iterations could cause the search process to end too soon and produce less-than-ideal results. Setting a high number of repetitions, however, may result in increased computing complexity and time consumption.

Computational efficiency and the requirement for adequate search space exploration must be balanced in order to determine the optimal number of iterations. It frequently necessitates trial and error, with the number of iterations adjusted according to the features and convergence behavior of the problem. Finding the right balance between limiting the number of iterations necessary for the algorithm to converge to a workable solution and minimizing needless computational overhead is crucial.

c.Random Numbers

The stochastic behavior of the PSO is attained by employing random values inside the interval [0, 1].

d.Velocity of the Particle

The important component in the PSO algorithm is velocity of the particle. Its value is limited by certain conditions. The parameters $\mathrm{v}_{\mathrm{max}}$ and $\mathrm{v}_{\mathrm{min}}$which specify which areas should be explored among the now and goal place, determine the fitness. This is because the particles move in larger stapes and the resultant solution could not be perfect. As well as, it takes longer for the particles to reach the necessary solutions because they are too small.

e.Velocity Components

Three factors affect the PSO algorithm's velocity update: social, cognitive, and inertia.

1. ωV_{ij}^{t}, the inertia component, is the agent's momentum or propensity to keep going in the same direction. It prevents abrupt direction changes and promotes smooth movement by being based on the agent's past velocity.

2. The cognitive component, represented by $c_1 r_{1j}^{t}(P_{best,i}^{t}\_x_{ij}^{t})$ is a reflection of the agent's unique experience or memory. It assesses the agent's historical performance and directs it toward achieving its own peak performance. This element pushes the agent toward settings that have historically produced good outcomes.

3. The social component explains the impact of a group of agents or the agent's neighborhood. It is expressed as $c_2 r_{2j}^{t}(G_{best}\_x_{ij}^{t})$ in gbest PSO and $c_2 r_{2j}^{t}(L_{best}_x_{ij}^{t})$in lbest PSO. It evaluates the effectiveness of nearby agents and directs the active agent to the greatest spot in its vicinity. By encouraging cooperation and information exchange among agents, this component enables them to come together as a group to find better answers. Velocity components of particle swarm optimization is shown in figure 3.10.

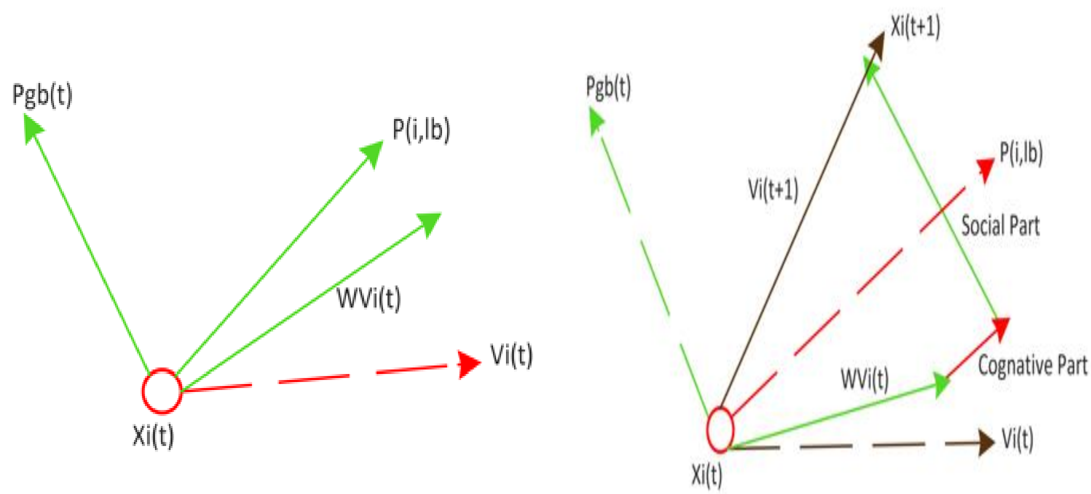

Figure 3.10 Velocity Components (Al-Shamma et al., 2018)

f. Acceleration Coefficients

The PSO algorithm uses the acceleration coefficients, c_1 and c_2, combined with randomly generated values, r_1 and r_2, to calculate the stochastic influence of the social and cognitive components of an agent's velocity.

The agent's self-confidence or unique memory is reflected in the acceleration coefficient c_1. When updating its velocity, it decides how much weight or significance is assigned to the agent's individual optimal position. An agent that has a higher c_1 value tends to rely more on its own best position and puts more faith in its own historical performance.

Conversely, the agent's trust in its neighbors, or the social component, is reflected in the acceleration coefficient c_2. When an agent's velocity is updated, it determines how much weight or priority is assigned to the best position discovered by nearby agents. A greater value of $c_2$means that the agent is more influenced by the optimal positions that its neighbors have found and trusts the collective knowledge of its neighbors more.

Stochasticity or randomness is added to the velocity update equation using the randomly generated numbers r_1 and r_2. By guaranteeing that every agent's velocity update is marginally different from the others, these random numbers encourage exploration and keep the algorithm from becoming locked in local optima.

The agent's confidence in its own performance and its dependence on the collective knowledge of its neighbors can be balanced by varying the values of $c_1$and c_2, which modifies the algorithm. The ideal combination for obtaining good convergence and exploration may need to be experimented with, as the optimal values of these coefficients vary on the particular issue being solved (Rehman et al., 2020).

The Properties of c_1 and c_2 are:

1.The social and cognitive components of the velocity equation vanish when $c_1 = c_2 = 0$.

The agents in this scenario will keep moving at their current pace without taking into account any information from their neighbors' best positions or their own personal best.

The velocity equation is updated as:

$$V_{ij}^{t+1}=\omega V_{ij}^{t} \tag{3.55}$$

The social and cognitive components practically vanish from the equation because they are multiplied by c1 and c_2,respectively, and both $c_1$and c_2 are set to 0.

The agents' inertia component ωV_{ij}^{t}, which indicates their momentum or propensity to keep going in the same direction, is the only factor that determines their velocity at the following iteration (t+1).

As a result, if both c_1 and $c_2$are set to 0, the agents will continue to move at their current speed until they encounter the search space's borders. Since the agents do not modify their velocity depending on their own best or the best positions found by their neighbors, this behavior may result in inefficient exploration and unsatisfactory solutions.

2. The social component based on neighbors' best positions becomes meaningless when $c_1 > 0$ and $c_2 = 0$, but the cognitive component based on own best has a non-zero value. Here, every agent behaves on its own, taking no information from its neighbors into account.

The velocity equation is updated as:

$$V_{ij}^{t+1}=\omega V_{ij}^{t}+c_1 r_{1j}^{t}(P_{best,i}^{t}-x_{ij}^{t}) \tag{3.56}$$

The only factor influencing the velocity update is the cognitive component, $c_1 r_{1j}^{t}(P_{best,i}^{t}-x_{ij}^{t})$. It displays the agent's self-assurance and prior achievements. Based on the difference between its present location (x_{ij}^{t}), and personal best position ($P_{best,i}^{t}$)multiplied by c_1 and a randomly generated value r_1, the agent modifies its velocity.

Consequently, each agent's velocity update is based only on its personal best position and the agent's confidence in its own performance when $c_1 > 0$ and $c_2 = 0$. Without taking into account any information from their neighbors, the agents operate autonomously, optimizing their placements based only on their own experiences. This may inhibit the algorithm's capacity for exploration and foster a lack of teamwork, which could lead to less-than-ideal results.

3. The velocity equation is updated exclusively by the social component, which is dependent on the best placements discovered by the agent's neighbors, when $c_1 = 0$ and $c_2 > 0$. In these cases, the cognitive component is rendered unnecessary.

The velocity equation is updated as

$$V_{ij}^{t+1} = \omega V_{ij}^{t} + c_2 r_{2j}^{t}(G_{best} \_ x_{ij}^{t}) \text{ for } g_{best} \text{ PSO} \quad (3.57)$$

$$V_{ij}^{t+1} = \omega V_{ij}^{t} + c_2 r_{2j}^{t}(L_{best,i} \_ x_{ij}^{t}) \text{ for } l_{best} \text{ PSO} \quad (3.58)$$

Here, the agents are drawn to a single point that is identified as $G_{best}$the best position discovered by the entire swarm. The global best position (G_{best}) minus the agent's current position (x_{ij}^{t}), multiplied by c_2 and a randomly generated value r_2, is how the agent modifies its velocity.

Hence, regardless of their unique experiences or individual best positions, every agent in the swarm will converge towards the global best position. This behavior encourages the agents to work together and share information because each agent is only affected by the swarm's aggregate knowledge. Strong convergence towards a single point may result from it, maybe offering a viable global solution. But it can also lead to early convergence and a lack of inquiry, particularly if the global best position turns out not to be the best answer to the given issue.

4. The average of the individual best positions ($P_{best,i}^{t}$) and the global best position (G_{best})will draw all agents in the swarm when $c_1 = c_2$.

The velocity equation is updated as:

$$V_{ij}^{t+1} = \omega V_{ij}^{t} + c_1 r_{1j}^{t}(P_{best,i}^{t} \_ x_{ij}^{t}) + c_2 r_{2j}^{t}(G_{best} \_ x_{ij}^{t}) \quad (3.59)$$

In this instance, the agents are impacted by both their individual and the global best positions, and the cognitive and social components are equally important. The agents modify their velocity according to the product of the difference, multiplied by c_1, between their current position (x_{ij}^{t}),and personal best position ($P_{best,i}^{t}$) and the difference, multiplied by $c_2$between their current position ((x_{ij}^{t}),and global best position (G_{best}).The velocity update equation becomes stochastic due to the random numbers$r_1$and r_2.

Consequently, the average position between each agent's personal best position and the global best position attracts them all. The agents' consideration of both their personal experiences and the swarm's collective knowledge promotes a balance between exploration and exploitation. It encourages group cooperation among the agents while still permitting some degree of solitary investigation. The swarm attempts to strike a balance between exploring new areas of the search space and taking advantage of promising locations by aggregating towards the average position.

5. In the velocity update equation, the social and cognitive components are substantially heavier when c_1>>c_2.This implies that each agent is largely guided by its own optimal location and gives less weight to optimal positions discovered by its neighbors.

The velocity equation is updated as:

$$V_{ij}^{t+1}=\omega V_{ij}^{t}+c_1 r_{1j}^{t}(P_{best,i}^{t}\_x_{ij}^{t})+ c_2 r_{2j}^{t}(G_{best}\_x_{ij}^{t}) \quad (3.60)$$

In this instance, the cognitive component has a greater overall influence on the velocity update due to the fact that $c_1$is substantially larger than c_2. The agents' velocities are varied by multiplying the difference between their present position (x_{ij}^{t}),and their personal best position ($P_{best,i}^{t}$) by c_1. The social component's contribution ($c_2 r_{2j}^{t}(G_{best}\_x_{ij}^{t})$)is very minor.

Because of this, each agent's past performance and current status have a significant impact. Because they are more interested in investigating their own unique experiences than in using the information provided by their neighbors, this may cause the agents to wander excessively. The swarm might work together less and be less able to converge on a global solution. Wandering too much can cause delayed convergence and possibly make it more difficult for the search to find the best answer quickly.

6. In the velocity update equation, the social component is given substantially more weight than the cognitive component when c_2>> c_1. This implies that each agent gives less weight to its own personal best position and is more influenced by the global best position determined by the swarm.

The velocity equation is updated as

$$V_{ij}^{t+1}=\omega V_{ij}^{t}+c_1 r_{1j}^{t}(P_{best,i}^{t}\_x_{ij}^{t})+ c_2 r_{2j}^{t}(G_{best}\_x_{ij}^{t}) \quad (3.61)$$

In this instance, the social component has a greater overall influence on the velocity update due to c_2 being substantially larger than c_1. The global best position (G_{best}) minus the agent's present location (x_{ij}^t),multiplied by c_2, determines the agents' velocities; in contrast, the cognitive component's contribution,($c_1 r_{1j}^t(P_{best,i}^t - x_{ij}^t)$)is very minimal.

Thus, each agent is greatly affected by the swarm's global optimum position. Premature convergence is a risk associated with this, in which all agents rapidly converge towards the global optima without thoroughly examining the search space or accounting for their unique experiences. If the global best position turns out not to be the genuine optimal solution, then the swarm may become less diverse and more prone to become stuck in local optima. Even if the swarm might converge more quickly on a solution, too much reliance on the global best position can stifle investigation and provide less than optimal outcomes. Achieving a balance between the cognitive and social components is crucial in order to maintain an appropriate exploration-exploitation trade-off and avoid premature convergence.

To achieve optimal results in the Particle Swarm Optimization (PSO) technique, it is crucial to initialize c_1 and c_2. Adverse assumptions or inadequate selection of these acceleration constants may result in undesired patterns, such oscillatory or cyclic behavior. Setting c_1 and c_2 to the same value, such as $c_1 = c_2 = 2$, is a typical PSO technique.

This option gives the social and cognitive aspects of the velocity update equation a balanced influence. When calculating the agent's velocity, equal weight is given to the optimal positions discovered by neighbors as well as the agent's own.

It's crucial to remember that the optimal values for c_1 and $c_2$can change based on the particular issue being resolved. Although $c_1 = c_2 = 2$ might be an effective answer in many situations, it is not a perfect solution and should only be used as a jumping off point for further testing and optimization.

The characteristics of the issue, the dimensionality of the search space, and the intended trade-off between exploration and exploitation are generally taken into consideration when determining the ideal values for $c_1$and c_2.

Finding the best choices for c_1 and $c_2$that result in good convergence and exploration qualities for a specific issue usually involves experimentation and parameter modification.

g. Termination criterion

The evaluation processes undergo several iterations and objective function tolerance beyond the initial phase or until stopping criteria is satisfied. The achievement of a predefined maximum number of iterations or a particular degree of precision in the solution is often the halting condition.

3.11 PSO Parameters Selection

A few tuning parameters for the PSO method include the inertia weight (w), particle number (m), acceleration constants ($c_1$and c_2), maximum limiting velocity (V_{max}), maximum number of iterations (T_{max}), and computed precision (ε).$T_{max}$and ε are utilized as the conditions to end the iteration, whereas w, m,c_1, c_2,and V_{max} are employed as the primary regulating factors (Yan et al., 2019).

3.11.1 Analysis of Inertia Weight Selection

The concept of inertia weight explains how past velocity affects present velocity. PSO's ability to search both locally and globally can be adjusted by managing its choices. Particle velocity depends on current position pbest (personal best) and gbest (global best) if w = 0. The velocity is memory less. If w is greater than zero, the particle will tend to explore new territory; the more w, the greater the particle's flight velocity, and it will also explore in longer steps. The particle will tend to focus on local exploitation the smaller the w and the smaller the particle's flight velocity. Currently, linearly decreasing weight is utilized more often as the inertia weight(Qin et al., 2016; Voltage et al., 2019).

$$W=w_{max}-\frac{w_{max}-w_{min}}{T_{max}}*t \tag{3.62}$$

Where $w_{max}$is the maximum inertia weight, and w_{min} is the minimum inertia weight, typically w_{max} =0.9, w_{min} = 0.4 ; t is current iteration number; $T_{max}$is the maximum iteration number.

3.11.2 Analysis of Acceleration Constant Selection

A little acceleration constant could cause the particle to stray into the goal region, but a big acceleration constant could cause the particle to move swiftly toward the goal area or even take off from it. According to Kennedy and Eberhart, excessive roaming in the search space is the outcome of a comparatively high cognitive component value as compared to a social component value. On the other hand, particles may rush toward the local optimal point too soon if the social component has a relatively high value. Furthermore, they recommended that the acceleration coefficients be both set to 2 in order to bring the mean of the two stochastic elements to unity. Later, Clerc came to the conclusion that c_1=c_2=2.05, while other researchers disagreed, concluding thatc_1=2.8 was the result of trials.

These studies have actually been limited to the use of partial problems. Thus, it hadn't made every field popular. Suganthan conducted research on a technique that would reduce both acceleration coefficients linearly over time, but he found that solutions with fixed acceleration coefficients of 2 work better. He did, however, propose through actual research that the acceleration coefficients shouldn't always equal 2 (Eltamaly, 2021).

3.11.3 Analysis of Particle number population selection

Several researchers came to the conclusion that as particle numbers exceeded 50, their impact on PSO was less. On the other hand, particle counts below 50 had a significant impact on PSO performance. According to the calculated complexity analysis, increasing the number of particles necessitates increasing the function evaluation, which in turn increases computation time and reliability at the same time.

3.11.4 Analysis of the max Velocity Selection

In order to reduce the likelihood that a particle would move out from its search space during the evolutionary process, its velocity is typically limited to a range. A particle's maximum restricted velocity is denoted byv_{max}. The particle may fly through the good solution if $v_{max}$is abnormally big, indicating that the velocity is not limited. PSO performance at that point is dependent on inertia weight; on the other hand, if $v_{max}$is too little, the particle might not explore the outer local optimal area of space. So, it quickly becomes the best in the area. For these reasons, a too large or tiny velocity may cause an algorithm's performance to decline(Jain et al., 2022)(Barrera et al., 2016).

3.12 Optimal Power Flow Problem Formulation

Finding the best control variable settings for power system components to minimize the chosen objective functions while meeting all equality and inequality requirements is the primary goal of OPF. Three objective functions are found in this work to solve OPF for the system.

3.12.1 Mathematical Modeling of Static Var Compensator (SVC)

The SVC is a shunt type FACTS device, which is described as a shunt linked static variable voltage generator or absorber whose output is modified to interchange capacitive or inductive current in order to maintain or manage certain power system characteristics, most commonly the bus voltage. At a selected bus, the SVC has the option to inject or absorb its reactive power (Q_{svc}). If $Q_{svc}$is less than zero, it adds reactive power to the system; if $Q_{svc}$is more than zero, it removes reactive power from the system (Devi & Padma, 2017). At node n, the injected power is:ΔQ_n=Q_{svc}.Structure and model of SVC is shown in figure 3.11 below.

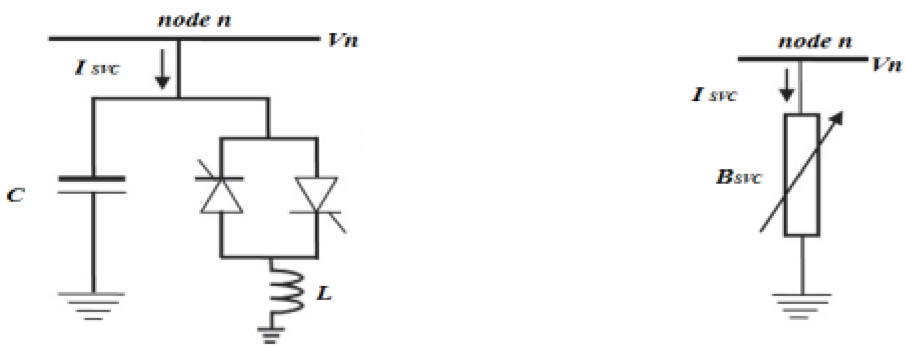

a. Structure of svc b. Model of svc

Figure 3.11 Structure and model of SVC(A. Optimization et al., 2022)

The current and reactive power of static var compensator exchanged with node n is is given by:

$$I_{svc}=jB_{svc} * V_n \tag{3.63}$$

$$Q_{svc=}Q_n=jB_{svc} * V_n^2 \tag{3.64}$$

The reactive power by generated by SVC is expressed as

$$Q_{min} \leq Q_{svc} \leq Q_{max} \tag{3.65}$$

The linearized equation is expressed by the following equation

$$\begin{bmatrix} \Delta P_i \\ \Delta Q_i \end{bmatrix} = \begin{bmatrix} 0 & 0 \\ 0 & Q_i \end{bmatrix} \begin{bmatrix} \Delta\theta_i \\ \Delta B_{svc/B_{svc}} \end{bmatrix} \tag{3.66}$$

The total SVC susceptance required to keep the nodal voltage magnitude at the given value is represented by the changing susceptance.

$$X_{svc}=\frac{X_c X_l}{\frac{X_c}{\pi}(2(\pi-\sigma)+\sin(2\sigma))-X_l} \tag{3.67}$$

$$B_{svc}=\frac{1}{X_{svc}} \tag{3.68}$$

By considering and an ideal case, the steady-state characteristic's slope (SL) would be zero. Thus, throughout the iterative phase of the load-flow computation, the network bus in which SVC is placed will be viewed as a generator bus (pv) where P=0 and V=V_{ref}

When SVC operates in the linear control domain:

$$I_{min} < I_{svc} < I_{max} \tag{3.69}$$

$$V_{min} < V < V_{max} \tag{3.70}$$

When SVC operates outside the linear control domain:

a.Capacitive operation, when $V < V_{min}$

b. Inductive Operation, when $V > V_{max}$

Certain sign rules concerning the meaning of absorbed/injected reactive power and the equivalent susceptance (B_{svc}) are adopted in order to create models that are compatible with steady-state computation:

a. $Q_{svc} > 0$ or$B_{svc} < 0$ indicates an inductive characteristic of the SVC, meaning it draws reactive power from the power system.

b. $Q_{svc} < 0$ or$B_{svc} > 0$ indicates an capacitive characteristic of the SVC, meaning it injects reactive power to the power system.

c. The susceptance value is computed as follows if the SVC needed current $I_{svc} > I_{max}$ which violates the inductive limit.

$$B_{min} = \frac{-Q_{max}}{V_{max}^2} \tag{3.71}$$

Where $Q_{max}(= QL_{max})$ is maximum inductive reactive power at V_{svc}=V_{max}, $Q_{max} > 0$

d. The susceptance value is computed as follows if the bus voltage $V < V_{min}$ which violates the capacitive limit.

$$B_{max} = \frac{Q_{min}}{V_{min}^2} \tag{3.72}$$

3.12.2 Formulation of Objective Function

The primary goal is to identify the best position and parameter configuration for the SVC in the power system to minimize the load voltage deviation and power system loss.

A. Voltage Deviations Minimization:

The electrical system's operation is affected by changes in voltage. In addition, the voltage supplied to the client needs to fall within a set range. Consequently, minimizing the voltage variations mentioned should be the primary goal function to take into account.

$$f_1 = V_d = \sum_{j=1}^{N} \left(V_{ref} - V_i\right)^2 \tag{3.73}$$

Where,V_i is Voltage at bus 'i' andV_{ref} is nominal voltage which is 1pu.

Nis total number of bus

B.Power Loss Minimization:

The feeder's radial distribution network's total active power loss is calculated as:

$$f_2 = \sum_{j=1}^{N_b} \left(R_j * I_j^2\right) \quad (3.74)$$

The feeder's radial distribution network's total reactive power loss is calculated as:

$$f_3 = \sum_{j=1}^{N_b} \left(X_j * I_j^2\right) \quad (3.75)$$

where the system's first and second objective functions, denoted by f_1 and f_2, stand for the minimization of reactive power loss and active power loss, respectively. N_b is the number of branches in the outgoing feeder, whileR_j,X_j, and $I_j$are the resistance, reactance, and current of branch j in the feeder,respectvily.

The following formulas can be used to determine the percentage of total active and reactive power loss.

$$\text{Total active power loss} = \frac{P_L - P_{svcL}}{P_L} * 100 \quad (3.76)$$

$$\text{Total reactive power loss} = \frac{Q_L - Q_{svcL}}{Q_L} * 100 \quad (3.77)$$

Where P_L and Q_L represent the total active and reactive power loss prior to the integration of the SVC device, and P_{svcL} and Q_{svcL}represent the total active and reactive power loss subsequent to the integration of the SVC device.

In general, the system's multiple objective function (MOF) can be changed to a single objective function using the equation below:

$$\text{Minimize (MOF)} = \text{Min} \left(w_1 * f_1 + w_2 * f_2 + w_3 * f_3\right) \quad (3.78)$$

Where w_1,w_2, and w_3 are the weighting factors, and the three objective functions define their magnitude. The three weighting components summation is unity.

3.12.3 Equality Constraint

Specific requirements must be met in order for equality restrictions to be met. Equations with the left side set to equal the right side are used to represent them. To enforce particular technical or operational criteria in the context of SVC placement, equality constraints might be applied.

$$P_g + \sum_{j=1}^{n} P_{svc} = \sum_{i=1}^{La} P_l + \sum_{j=1}^{N} P_{loss} \quad (3.79)$$

$$Q_g + \sum_{j=1}^{n} Q_{svc} = \sum_{i=1}^{Lr} Q_l + \sum_{j=1}^{N} Q_{loss} \quad (3.80)$$

$P_g$and $Q_g$define the real and reactive power of the generators at substation respectively, $P_l$and $Q_l$define the active and reactive power of load respectively and n is number of SVC unit,La,Lr represents number of active load and reactive load respectively.

3.12.4 Inequality Constraint

Contrarily, inequality restrictions are requirements that must be met within predetermined ranges. These are expressed as inequality symbols like "≤" (less than or equal to) or "≥" (greater than or equal to), which compare the left and right sides of the inequality. Physical or operational limits can be imposed using inequality constraints in the context of SVC placement optimization. To avoid overloading, for example, an inequality constraint may limit the maximum amount of power that can pass via a distribution line.

A.Number SVC constraint:

Aim to decreases the quantity of SVC placements.As such, the optimal number of SVC placements need to be smaller than or equivalent to the total number of locations.

$$N_{svc} \leq N_{svcmax} \tag{3.81}$$

B.SVC size constraint:

To attain the proper solution, the Static Var compensator's size shouldn't be either too small or large in relation to the load. The system's reactive power injection by SVC is constrained by the following lower and upper bounds:

$$Q_{svc}^{min} \leq Q_{svc} \leq Q_{svc}^{max} \tag{3.82}$$

C.Total reactive power constraint:

The total reactive power injection (Q_{svc}^{tot}) must be less than or equal to the total load reactive power (QL^{tot}).

$$Q_{svc}^{tot} \leq QL^{tot} \tag{3.83}$$

D.Bus voltage constraint:

All bus voltage should be within acceptable limits.

$$V_i^{min} \leq V_i \leq V_i^{max} \tag{3.84}$$

$$0.95 \leq V_i \leq 1.05$$

Where V_i voltage of the i^{th} bus

E. Load rating constraint:

The current rating is either less than or equal to the maximum rating.

$$I \leq I_{max} \tag{3.85}$$

F. Injected reactive power limit:

The Static Var Compensator's (SVC) reactive power must be defined within an acceptable range. The SVC's reactive power and the reactive load should be equal or less.

$$\sum_{j=1}^{Nsvc}\left(Q_{svc(j)} \leq Q_{L(j)}\right) \quad (3.86)$$

Where$Q_{svc}$is reactive power generated by the SVC unit and Q_L is reactive load.

G. Injected active power limit:

Active power generated by the Static Var Compensator (SVC) is must be defined to acceptable range. The SVC's active power and the active load should be equal or less.

$$\sum_{j=1}^{Nb}\left(P_{svcj} \leq P_{Lj}\right) \quad (3.87)$$

3.13 Utilization of PSO Algorithm to determine the size and Location of SVC

The location representation of each individual in the m-dimensional search space used in particle swarm optimization is denoted by particle (X_i), as seen below.

$$X_{i=}(x_{i1}, x_{i2}, x_{i3} \ldots . x_{im}) \quad (3.88)$$

The position and capacity of the SVC were utilized as the dimensions of the search space in this study, as indicated below.

$$X_{i=}(c_{ij}, l_{ij}) \quad (3.89)$$

where i and j represents particle number and number of SVC respectively.

Initializing the position of the swarm or particles is the first phase in the PSO implementation process. As a result, the location, size, and number of SVCs are the decision factors (control variables) for this study.

The Multiple Objective Function can be expressed as follows:

MOF=min ($w_1 * f_1$+$w_2 * f_2$+$w_3 * f_3$)

Step 1: Select the variables that need to be optimized using PSO. In this case, the variables are the real and reactive power that is injected into the distributed system using SVC, or the SVC's size, in order to reduce losses and enhance the voltage profile.

Step 2: Select the swarm's size.

Step 3: Provide the SVC size's random values.

Step 4: Run the load flow to find the system's losses and voltage profile.

Step 5: Additionally, use PSO to find the SVC's proposed placement.

Step 6: Since we want to determine the ideal SVC size to reduce the losses as much as possible, let's assume that the fitness function represents the true loss.

Step 7: Set the swarm's initial position and speed at random.

Step 8: Compute and store the fitness function of each particle in the swarm by placing various sizes of SVC at the place determined by PSO.

Step 9: Let Pbest be the original SVC sizes that were generated at random.

Step10: The particle with the least amount of loss is regarded as the gbest after iterating through all of the fitness function values.

Step 11: Set the acceleration coefficients to c_1=2 and c_2=2 at initialization.

Step 12: Set the loop's initial iteration count. Compute and update the position and velocity for every particle.

Step 13: After setting SVC, run the load flow to get the updated fitness function for every particle. Particles for which the new fitness value exceeds the prior pbest value have their pbest value set to the current fitness value. In a similar manner, the most recent pbest values are used to determine the gbest value.

Step 14: When the loop reaches the maximum number of iterations, stop it and plot the results. If not, proceed to step 12 and increase the number of iterations.

Step 15:SVC size is indicated by gbest value. Based on the outcome, we can say that by installing the right size of SVC, which is achieved by utilizing PSO, losses are significantly decreased and the voltage profile is enhanced. Flow chart of PSO based optimal Placement and sizing of SVC is shown in figure 3.12.

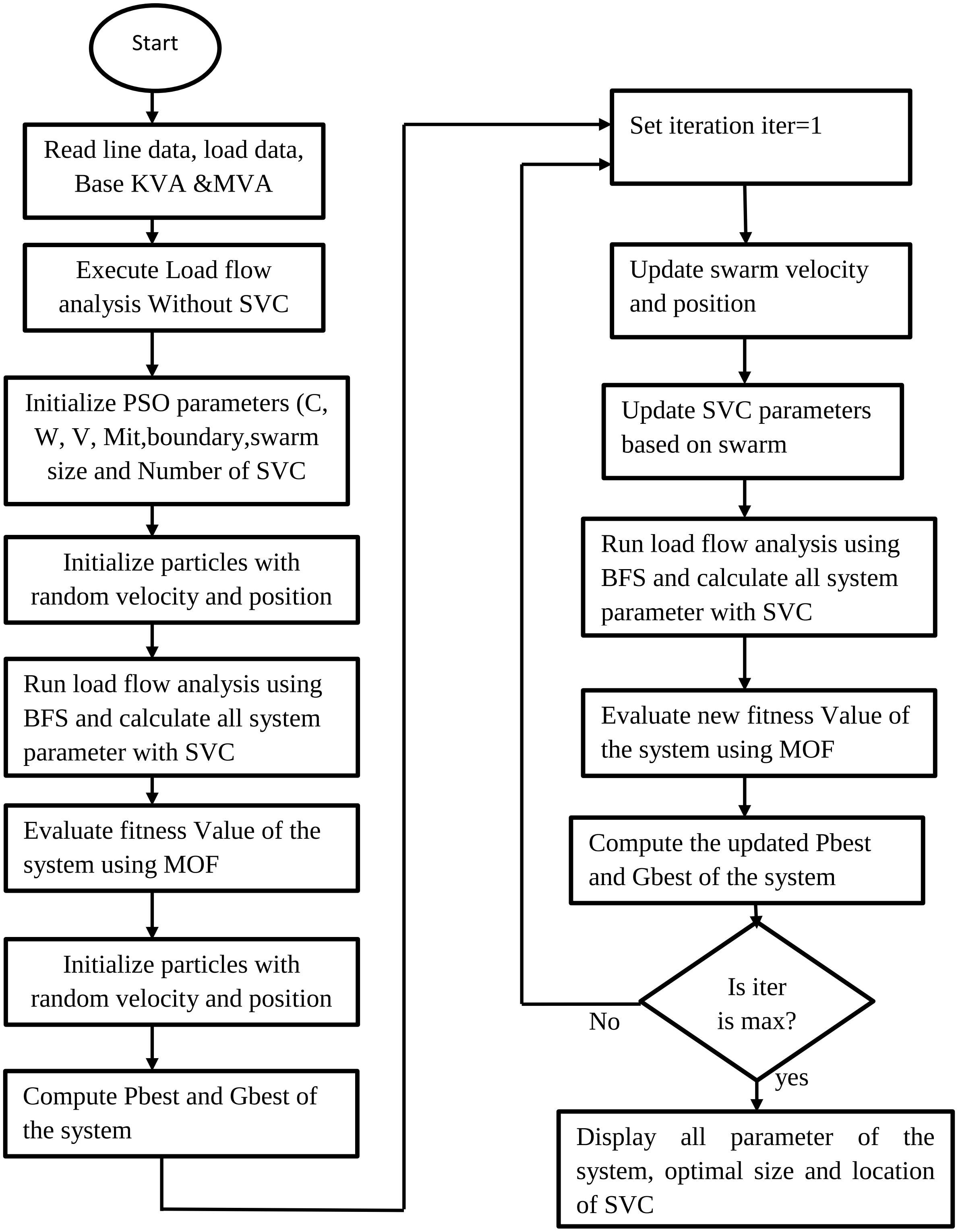

Figure 3.12 Flow chart of PSO based optimal placement and sizing of SVC

CHAPTER FOUR

4. RESULTS AND DISCUSSIONS

This chapter presents the results and optimization process obtained from MATLAB 2018a Software environment by considering different scenarios (two scenarios): one involving the incorporation of SVC and the other was without it. OPF is performed to examine power loss, costs concern, voltage profile, and voltage stability with and without the installation of SVC in the system. The base value was 15kV and 100MVA, and the maximum and minimum voltage limitations were determined to be 1.05pu and 0.95pu, respectively, in order to properly carry out the forward/backward power flow program.

PSO is used in the MATLAB Software to choose the possible busses. The optimal SVC size has been determined using these candidate buses and various SVC values as input. The optimal size of SVC obtained by particle swarm optimization is 2500.51KVAr. The electric power supply network incorporates with the first bus whereas, radial distributions feeder incorporated with all the other buses considered for allocating SVC of the specified size from the range.

Power losses, voltage profiles, and loss costs are examined with and without the inclusion of SVC using load flow analysis. The PSO technique is used as a decision-making tool to establish the optimal size and position of SVC at a time of integration. In general, the base case and the integration of the optimal SVC size and position are examined in relation to the parameters that impact the distribution system's performance on, voltage profile, active and reactive power losses.

To choose the greatest performance enhancement scenario, two distinct scenarios are created from the current system and examined separately.

a) Base case or Existing system (Case_1)
b) With SVC integration (Case_2)

4.1 Case I: Base Case or Existing System

4.1.1Base Case Active Power Loss Result

The LFA was performed using BFS methods to determine the feeder's present condition. Prior to the incorporation of the SVC to the feeder, the active and reactive power loss was calculated. The line and bus data from table appendix –d have been used as inputs for the BFS algorithm. The inputs must be converted to per-unit values before the algorithm runs by setting the base voltage to 15 KV and the base MVA to 100. There are 11.335 MW and 7.941 MVAr of total active and reactive load demands on the feeder, respectively. According to the simulation results, the system has a total reactive power loss of 350.081 KVAr, but a total real power loss of 401.432 KW.The feeder has huge amount of losses and it is not economical to lose such amount of power. A distribution system needs the least amount of power loss possible to maintain proper system conditions, and the feeder needs to be significantly improved in order to minimize the losses. Base case active power loss of Gefersa 14 feeder is shown in figure 4.1 below.

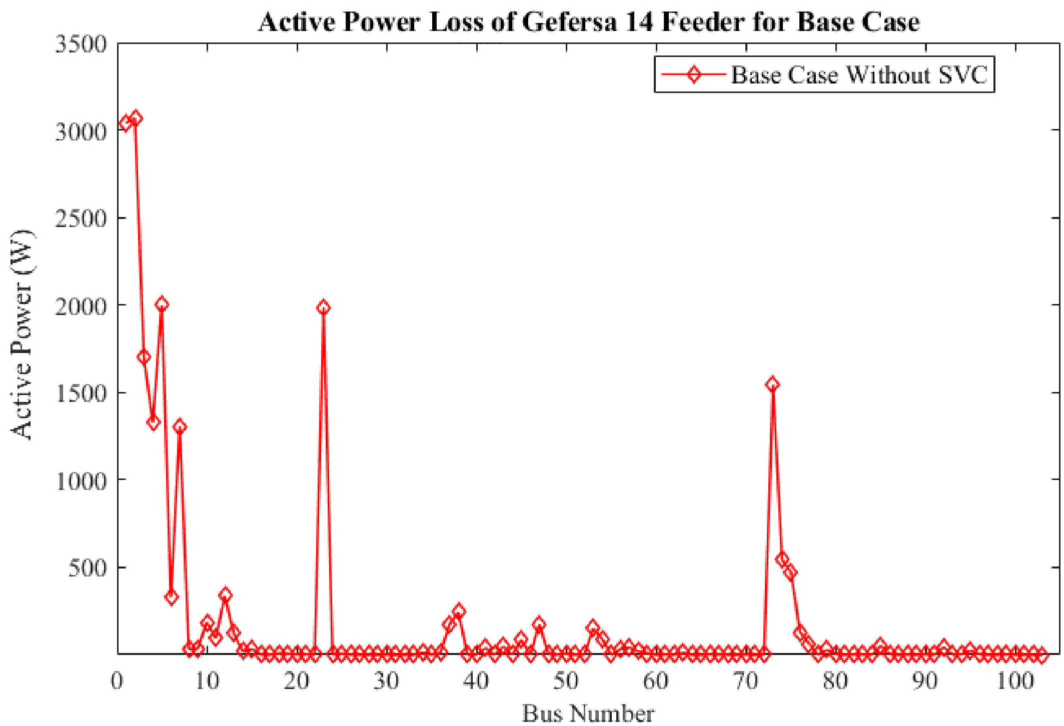

Figure 4.1 Active power loss of Gefersa 14 feeder

4.1.2 Base Case Reactive Power Loss of Gefersa 14 Feeder

Reactive power plays a critical role in the distribution feeder to maintain the voltage needed to increase active power flow through the line. Reactive power and line voltage have a direct relationship as well as voltage is used in the line to push the power through the line. As reactive load increases, the feeder voltage is going to decrease. Since most of the distribution load is inductive, the reactive power is needed on the side of distribution.

As a result, the feeder's reactive power losses significantly affect how well active power is delivered in the line and voltage profile at each node. The reactive power loss in line of the feeder-14 Gefersa substation is shown in figure 4.2 below. The BFS approach is used to find the simulation result prior to the distribution static compensator installation. Consequently, 350.081kVAr is the total reactive power loss. Reducing this reactive loss will help to keep the system working at optimal levels. Reactive power compensator has been used in this thesis to decrease reactive power losses.

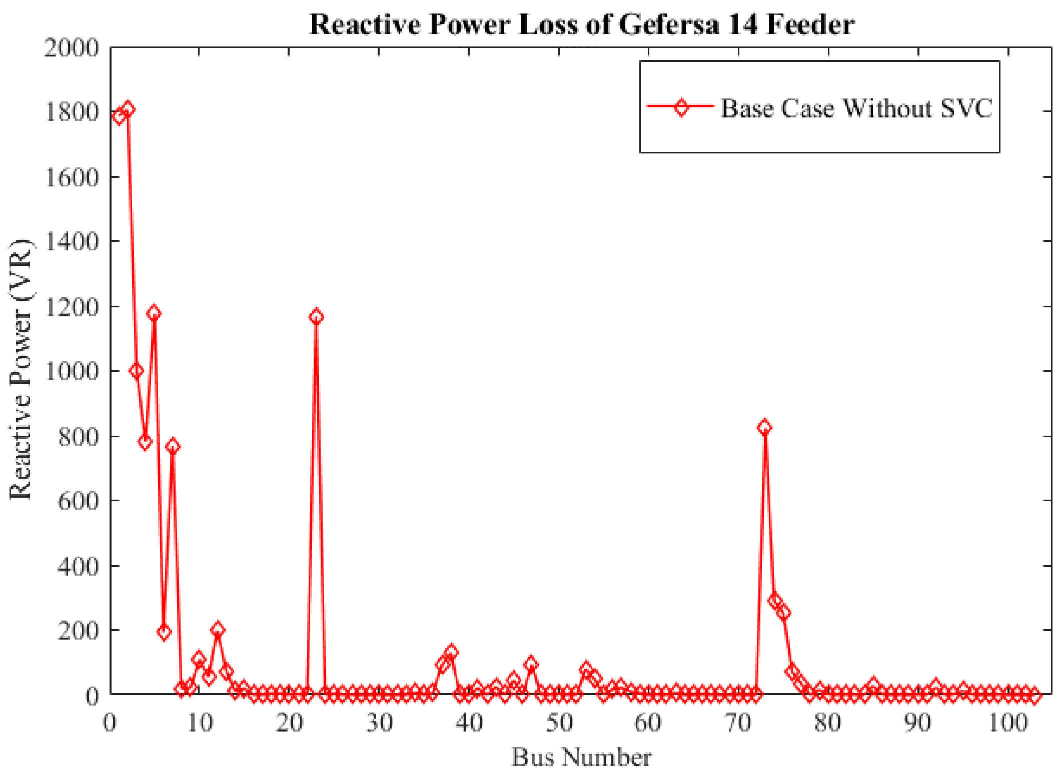

Figure 4.2 Reactive power loss before compensation

4.1.3 Base Case Voltage Profile Result

Before SVC integration, the base case voltage profile at each bus of the feeder is also calculated using the forward-backward load flow method, and its value is obtained. The minimum voltage value is 0.7 at bus 80 which is below the limit of 0.95pu and forty-one buses are below the allowable voltage range. Based on the distance traveled and the loading of the line, the voltage profile of the feeder is determined by the voltage value obtained during load flow. The observed voltage drops increase with feeder length; the voltage value of the nodes close to the source is higher than the voltage magnitude far from the generation; the obtained voltage magnitudes require refinement in order to increase the feeder's capacity for power flow.

From the perspective of power systems, a voltage profile of the distribution system needs to be improved to the standard voltage profile. Enhancing the voltage profile of the distribution reduces power losses and improves system performance. This appropriate placement and size of SVC on the buses can raise the voltage level to the required standard. Base case voltage profile of Gefersa 14 feeder is shown in figure 4.3 below and table 4.1 shows base case simulation results of Gefersa 14 feeder.

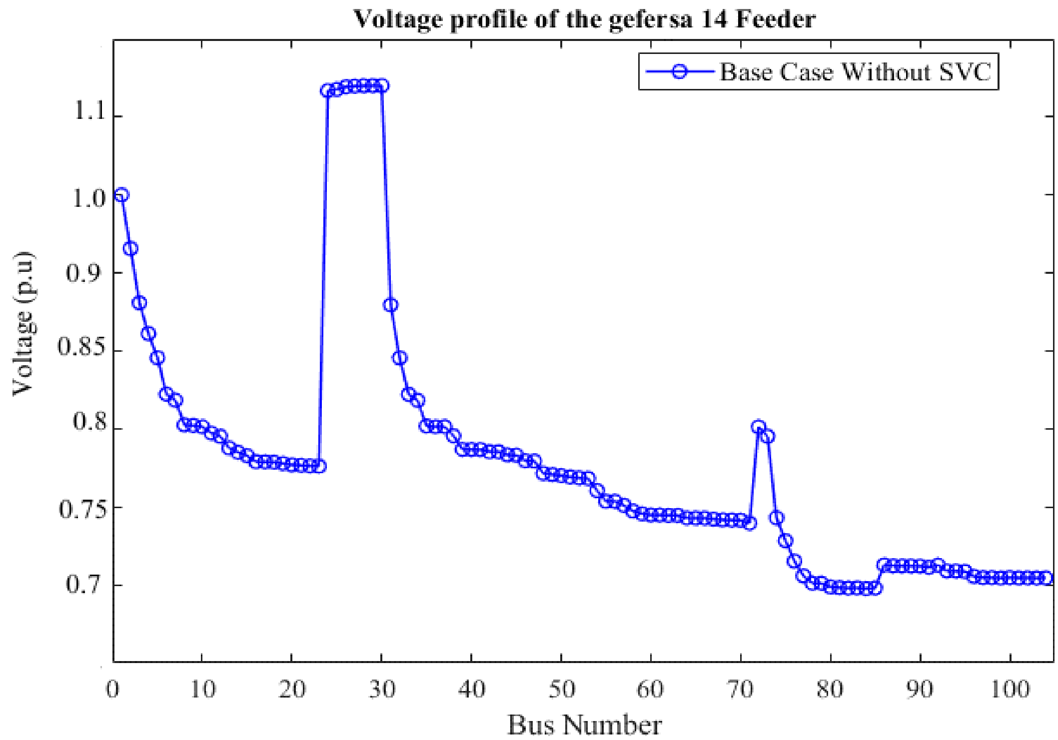

Figure 4.3 Base case Voltage profile of Gefersa 14 feeder

Table 4.1 Base case results of Gefersa-14 feeder

Parameters	Base case results
Total active power loss (KW)	401.432
Total reactive power loss (kVAr)	350.081
Minimum Voltage (pu)	0.7

4.2 Load flow results after Integration of Static Var compensator

The effects of SVC incorporation to distribution lines are examined in the thesis work in order to modify the line losses, and voltage profile of each bus system. Depending on the quantity and size of the connected device, analysis of both active and reactive power losses, as well as improvements to the voltage profile of the feeder, have been done in this instance. As stated in the thesis, the primary goal was to improve the performance of distribution lines, with a particular emphasis on minimizing power loss and boosting voltage profile, as well as evaluating the effects of SVC each feeder bus. The focus of this inquiry is the Gefersa substation outgoing feeder, and all relevant feeder data, such as line and bus data.

4.2.1Active Power Loss with Integration of SVC

The active power loss decreased from 401.432KW to 229.208KW after SVC was installed in the feeder. This means that loss was minimized by 172.224 KW and the active power loss was reduced by 43% when the device was properly sized and assigned to the selected bus. PSO algorithm was used to estimate the device's size and place; the optimum values are 2500.51kVAr for the device's size and bus 82 for its placement. Therefore, the saved power loss large amount that could produce various goods to meet societal demands, it could not be considered a negligible amount of money. The conserved electricity is crucial to change Ethiopia's economy, particularly in light of the country's developing condition. By decreasing the frequency and duration of interruptions, the feeder can become more dependable for the client due to the decreased loss. Figure 4.4 shows the power losses of the current feeder with a single SVC. It is evident that over all line segments, real power losses have been kept to a minimum.

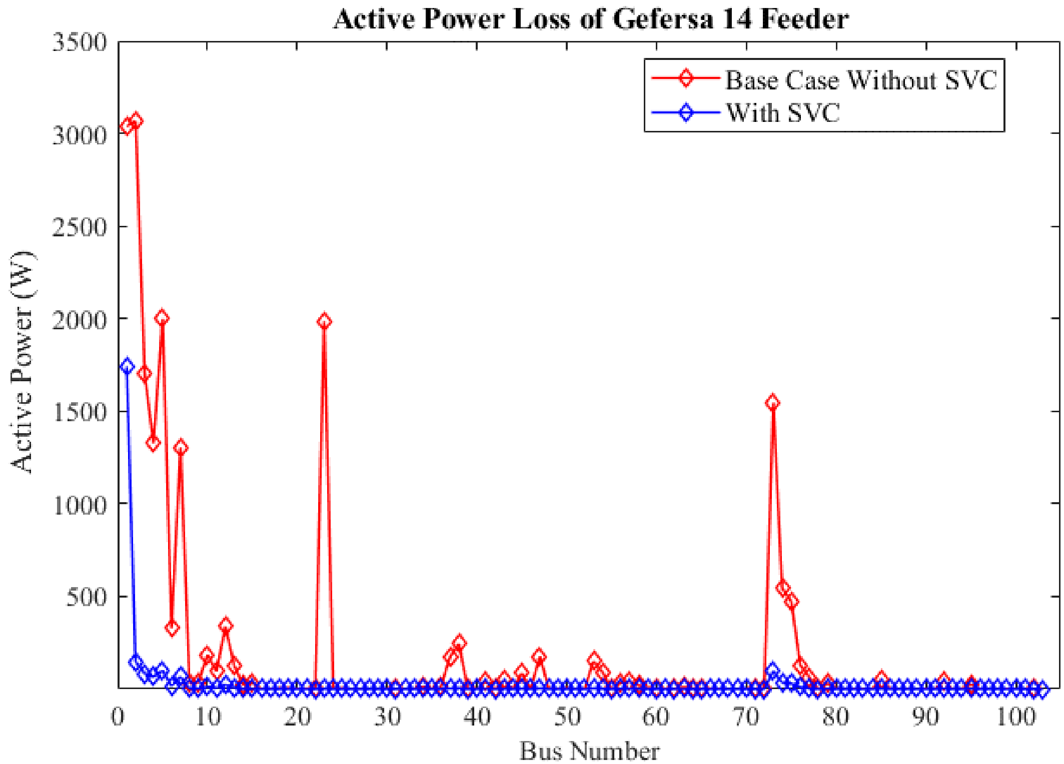

Figure 4.4 Active power losses reduction with incorporation of SVC

4.2.2 Reactive Power Loss with Integration of SVC

Maintaining the distribution system's voltage magnitude is crucial to the efficient operation of the system in order to lower losses and regulate the system's capacity to tolerate and prevent voltage collapse. Because reactive power and operational voltage are closely correlated, having too little reactive power lowers the voltage while having too much reactive power increases the system's voltage profile. In this instance, SVC has been used, and the outcome demonstrates a greatly reduced reactive power loss that can maintain the stability of the system. Reactive power loss was reduced from 350.081KVAr to 216.722KVAr, representing a 38% reduction, following the inclusion of SVC in the feeder. The reduced reactive power loss in the feeder following the incorporation of the SVC is shown in figure 4.5.

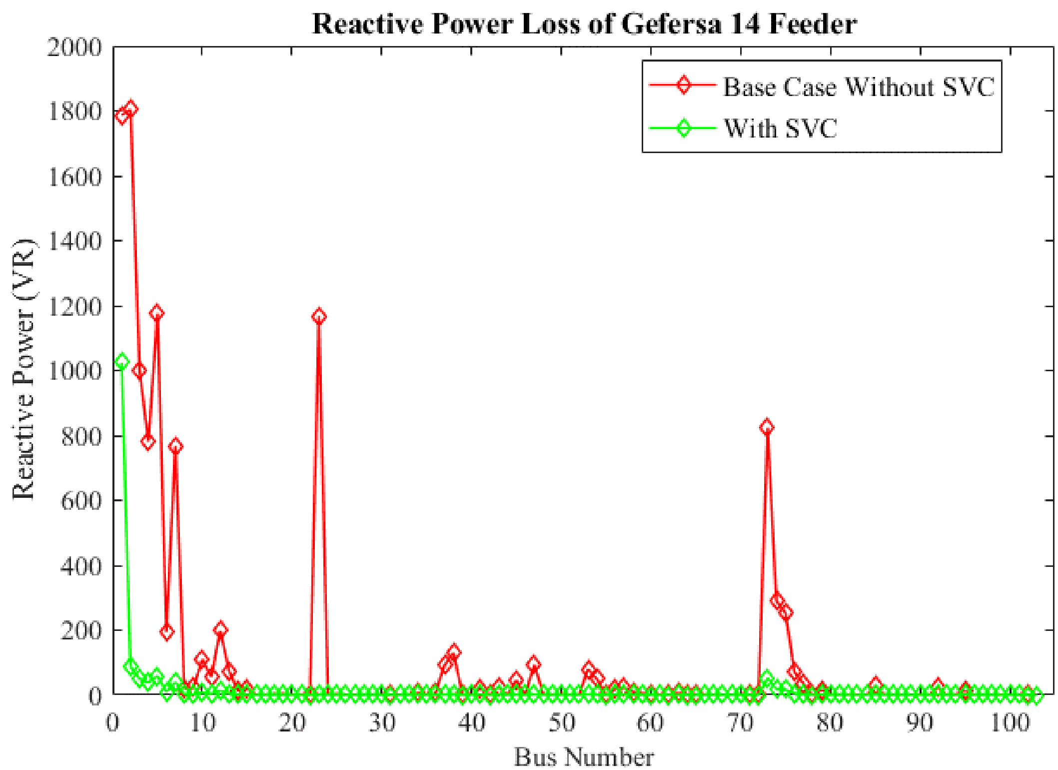

Figure 4.5 Reactive power losses reduction after incorporation of SVC

Figure 4.6 shows the total real and reactive power loss in the feeder with and without a SVC. It is evident that, following the incorporation of SVC, the total real and reactive loss in every line segment is lower than it was prior to the consideration of static Var compensators.

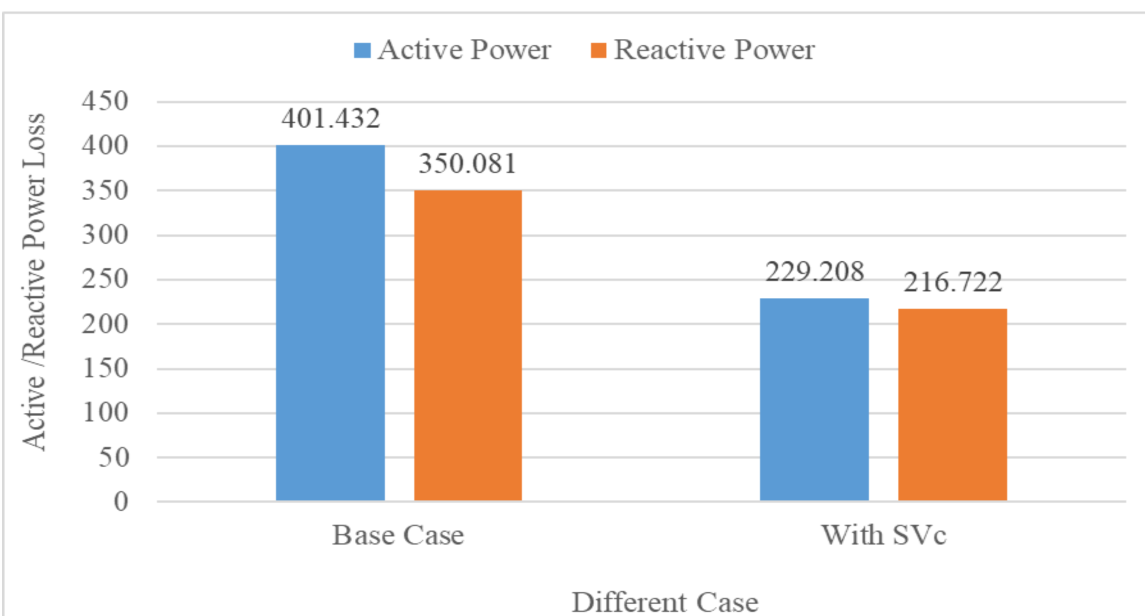

Figure 4.6 Active and reactive power losses with and without SVC

Table 4.2 below includes information such as location, size, number of SVC, active and reactive power loss, percentage reduction of active and reactive power losses, explains the overall simulation result that is found after injecting reactive power at the proper place.

Table 4.2 Power losses simulation results after integration of SVC

Parameters	without SVC	with SVC
Location	-	@82
Size(KVAr)	-	2500.51
Number of SVC		1
Active power loss(KW)	401.432	229.208
Reactive power Loss(KVAr)	350.081	216.722
%Reduction active power loss	-	43%
%Reduction in reactive power loss	-	38%

4.2.3 Voltage Profile Improvement after Incorporation of SVC

With optimum Place and appropriate size, the SVC can be incorporated at the distribution feeder with the goal of reducing power loss and improving voltage profile. The bus system displays a weak voltage profile at certain buses that is insufficient at the distribution system, as can be observed from the base case system following the use of load flow analysis.

Prior to the device's adjustment, bus 80 minimum voltage value was approximately 0.7, which is practically outside of the permitted voltage range according to IEEE standards. Therefore, voltage profile at bus 80 has improved from 0.7 to 0.9601 after the SVC was incorporated at the appropriate node by PSO. This is better than the voltage value obtained prior to the SVC incorporation, and bus voltage profiles have also been enhanced.

As the voltage profile simulation result makes clear, bus 80 voltage value and that of its surrounding buses are improved. The voltage profile improvement attained following SVC incorporation is seen in figure 4.7.

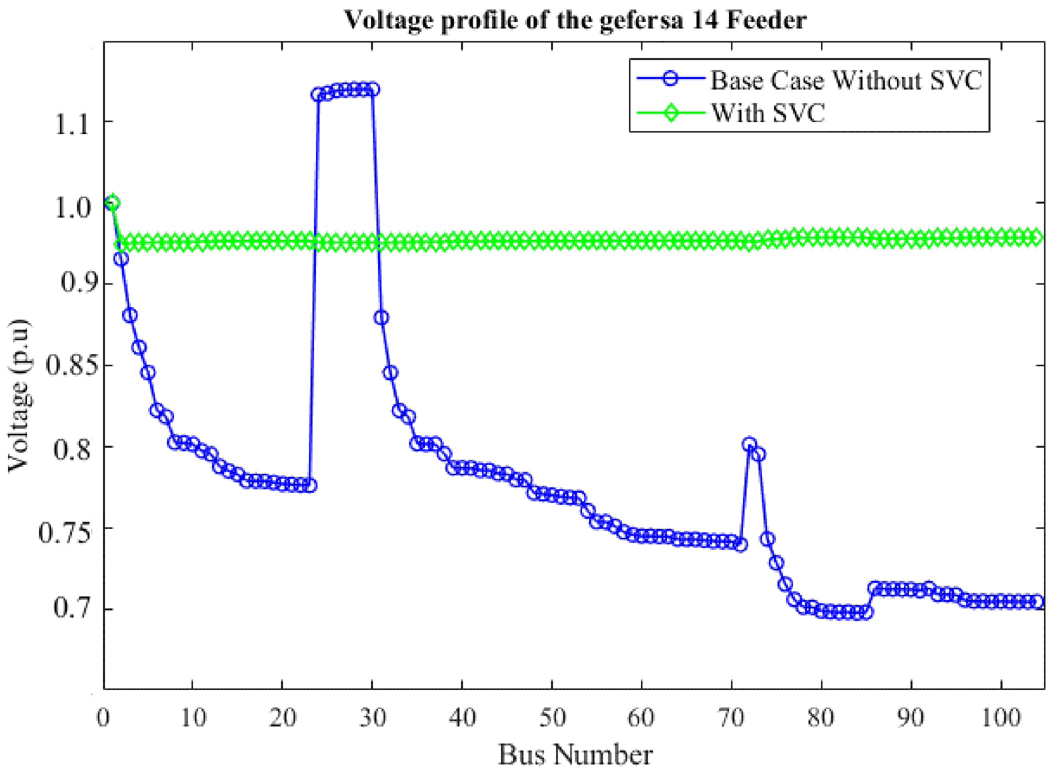

Figure 4.7 Voltage Profile of the Gefersa 14 feeder with Svc

4.3 Total Annual Cost Saving and Installation of SVC

One essential stage is to determine the economic feasibility of a proposed solution to a problem. Savings cost, or the difference between the cost of energy losses in birr before and after integration of the devices, is used to calculate the cost-effectiveness of those devices' integration in Gefersa-14 feeder. This thesis work's cost analysis takes into account the cost of SVC, the cost of energy lost or interrupted, and the overall cost savings with a payback period under the best-case.

A.Annual Energy Loss

The energy cost associated with the disruption and loss of the Gefersa-14 feeder prior to the installation of the SVC (case-1) can be computed as follows.

Annual Energy Loss of Gefersa -14 Feeder $=P_{loss}$*8760hrs (4.1)

=401.432*8760 = 3,516,544.32kwhrs

B.Cost of Power Loss

The cost of power loss in the outgoing feeder can be calculated as:

CEL= (Total active power loss of the feeder)*(E_c*t) birr (4.2)

Where,t=8760hrs

The average of the general tariff and 6th block rate, as indicated in Appendix C, is 2.4050 birr/ kwh under the new EEU tariff.

Cost of Energy Loss =AEL*2.4050 birr/kwh

=3,516,544.32kwhrs*2.4050birr/kwh

=8,457,289.09birr

Following this integration, the feeder's power loss drops to 229.208KW, resulting in an annual cost reduction of 4,828,929.37 birr for energy loss. This demonstrates that SVC is integrated in the feeder at the optimal size and placement; 3,628,359.72 birr may be saved annually.

The cost function of Static Var Compensator is given by:

C_{svc}=0.0003Q^2-0.3051Q+127.38USD/KVAR (4.3)

=0.0003(2500.51^2) – 0.3051(2500.51)+127.38

=61.655USDT/KVAR

Where Q=Q_{max}-Q_{min},operating range of SVC in MVAR.

The total installation cost of static var compensator if given by:

IC =C_{svc}*Q*1000,where C_{svc} is the cost of SVC in USD/KVAR (4.4)

=61.655*2500.51*1000

=74,017,444.05USD

The average value of installation cost for five years is given by:

$C_{av}=\frac{IC}{8760*5}$USD/hr =1,689.89USD/hr

5.CONCLUSIONS AND RECOMMENDATIONS

5.1 Conclusions

The distribution system's primary issues that impact performance are power outages, low voltage profiles, high power interruptions, distorted voltage and current at the customer's end, and unstable voltage in the system node; to address these issues, a technical solution is needed. During this study, the appropriate size and location of the SVC have been used to address power issues that arise in the distribution network. This study has employed particle swarm optimization (PSO), load flow analysis as fundamental techniques. Before and after the integration of Static Var Compensator, each bus voltage as well as the active and reactive power losses were determined using a backward-forward load flow analysis method. The PSO was utilized to determine the optimal placement and dimensions for the devices. The Gefersa distribution substation's feeder F14 (Gefersa 14) is selected from the feeders. There are 103 buses and 102 branches.

Multi objective function was formulated in this thesis including voltage profile enhancement, real and reactive power loss reduction by using Optimal size and location of SVC using PSO algorithm. By using optimal power flow backward/forward load flow analysis at base case the power loss and the voltage of each bus is obtained. From the result of base case real and reactive power loss are 401.432 KW and 350.081 respectively and the minimum voltage is formed at bus 80 which is 0.7. By using appropriate size and location of SVC with PSO the size is 2500.51KVAr and location is at bus 82. After integration of static Var compensator real and reactive power loss is reduced to 229.208kw and 216.722kvar respectively and also minimum bus voltage is improved to 0.9601. Following this integration, the feeder's real and reactive power loss reduced by 43% and 38% respectively, resulting in an annual cost reduction of 4,828,929.37 birr for energy loss. This demonstrates that SVC is integrated in the feeder at the optimal size and placement; 3,628,359.72 birr may be saved annually.

5.2 Recommendations

By reducing real and reactive power loss in a power system, this is great advantages for Ethiopian electric utility and customers. Thus, lower losses will make it possible to satisfy societal needs, reduce the amount of money wasted as a result of losses and improve voltage level to the required standard. Therefore, applying this strategy in the Gefersa distribution network would be beneficial, and I strongly advised Ethiopian Electric Utility to do so.

5.3 Suggestions for Future work

It is impossible for a scientific investigation to look into every angle and important topic at once; certain topics will have to wait for further research. These are some possible directions for future study.

- While phase-balanced loading conditions have been taken into account in this thesis, but phase imbalance and harmonics is not considered in this thesis.
- Utilize other algorithm for optimal performance and compare the PSO outcome to that of another optimization algorithm.
- Other power system elements, such as the short circuit level and other stability concerns, can be taken into account in the future objective function.
- Utilize other FACTS device and compare their performance with SVC.

REFERENCES

Access, O. (2022). *VOLTAGE STABILITY ENHANCEMENT USING STATIC VAR COMPENSATOR*. *04*.

Adebisi, O. I., Adejumobi, I. A., Ogunbowale, P. E., & Ade-Ikuesan, O. O. (2017). Application of Static Var Compensator for Voltage Stability Enhancement and Power Loss Reduction in Power System Networks. *LAUTECH Journal of Engineering and Technology*, *11*(2), 46–58.

Al-Shamma, B. R., Gosselin, O., & King, P. R. (2018). History matching using hybrid parameterisation and optimisation methods. *Society of Petroleum Engineers - SPE Europec Featured at 80th EAGE Conference and Exhibition 2018*, *May*. https://doi.org/10.2118/190776-ms

Albatsh, F. M., Mekhilef, S., Ahmad, S., Mokhlis, H., & Hassan, M. A. (2015). Enhancing power transfer capability through flexible AC transmission system devices: a review. *Frontiers of Information Technology and Electronic Engineering*, *16*(8), 658–678. https://doi.org/10.1631/FITEE.1500019

Asif, A., Ijaz, A., Urooj, A., Khan, T., & Munir, A. (2023). Voltage Collapse Prediction Using Artificial Neural Network †. *Engineering Proceedings*, *46*(1). https://doi.org/10.3390/engproc2023046024

Barrera, J., Álvarez-Bajo, O., Flores, J. J., & Coello, C. A. C. (2016). Limiting the velocity in the particle swarm optimization algorithm. *Computacion y Sistemas*, *20*(4), 635–645. https://doi.org/10.13053/CyS-20-4-2505

Bimali, B., & Pandey, R. (2022). *VAR Compensation On Load Side Using Thyristor Switched Capacitor and Thyristor Controlled Reactor VAR Compensation on Load Side using Thyristor Switched Capacitor and Thyristor Controlled Reactor*. *April 2021*. https://doi.org/10.3126/jie.v16i1.36568

Chaurasiya, K., Rajput, S., Parmar, S., & Patel, P. A. (2018). Reactive Power Management Using TSC-TCR. *International Research Journal of Engineering and Technology (IRJET)*, *5*(4), 1427–1431.

Chethan, M., & Kuppan, R. (2024). A review of FACTS device implementation in power systems using optimization techniques. *Journal of Engineering and Applied Science*, 1–36. https://doi.org/10.1186/s44147-023-00312-7

Conte, F., Massucco, S., Paolone, M., Schiapparelli, G. P., Silvestro, F., & Zuo, Y. (2020). Frequency stability assessment of modern power systems: Models definition and parameters identification. *Sustainable Energy, Grids and Networks*, *23*. https://doi.org/10.1016/j.segan.2020.100384

Devi, H. A., & Padma, S. (2017). *Optimal Location and Parameter Setting of FACTS Devices based on WIPSO and ITLBO for Power System Security Enhancement under Single Contingency*. *8958*(6).

Dhanalakshmi, C. (2022). Optimal Siting and Sizing of D-Statcom Using Particle Swarm Optimization. *International Research Journal of Engineering and Technology*, 1600–1606. www.irjet.net

Dhivya, S. (2020). *Reactive power compensation and bus voltage regulation using thyristor switched capacitor*. *96*(2), 4199–4205.

Eltamaly, A. M. (2021). *A Novel Strategy for Optimal PSO Control Parameters Determination for PV Energy Systems*.

Engelbrecht, A. P. (2016). *Particle Swarm Optimization : Global Best or Local Best ? 1*. https://doi.org/10.1109/BRICS-CCI-CBIC.2013.31

Gadal, R., Oukennou, A., Mariami, F. El, Belfqih, A., & Agouzoul, N. (2023). *Voltage Stability Assessment and Control Using Indices and FACTS : A Comparative Review*. *2023*.

Hamour, H., Kamel, S., Nasrat, L., & Yu, J. (2019). Distribution Network Reconfiguration Using Augmented Grey Wolf Optimization Algorithm for Power Loss Minimization. *Proceedings of 2019 International Conference on Innovative Trends in Computer Engineering, ITCE 2019*, *February*, 450–454. https://doi.org/10.1109/ITCE.2019.8646595

Hatziargyriou, N., Milanovic, J., Rahmann, C., Ajjarapu, V., Canizares, C., Erlich, I., Hill, D., Hiskens, I., Kamwa, I., Pal, B., Pourbeik, P., Sanchez-Gasca, J., Stankovic, A., Van Cutsem, T., Vittal, V., & Vournas, C. (2021a). Definition and Classification of Power System Stability - Revisited & Extended. *IEEE Transactions on Power Systems*, *36*(4), 3271–3281. https://doi.org/10.1109/TPWRS.2020.3041774

Hatziargyriou, N., Milanovic, J., Rahmann, C., Ajjarapu, V., Canizares, C., Erlich, I., Hill, D., Hiskens, I., Kamwa, I., Pal, B., Pourbeik, P., Sanchez-Gasca, J., Stankovic, A., Van Cutsem, T., Vittal, V., & Vournas, C. (2021b). Definition and Classification of Power System Stability - Revisited & Extended. *IEEE Transactions on Power Systems*, *36*(4), 3271–3281. https://doi.org/10.1109/TPWRS.2020.3041774

Herwan, M., & Mustaffa, Z. (2022). Results in Control and Optimization Optimal placement and sizing of FACTS devices for optimal power flow using metaheuristic optimizers. *Results in Control and Optimization*, *8*(June), 100145. https://doi.org/10.1016/j.rico.2022.100145

Idris, M. B. (2023). Study of Voltage Stability. *Iarjset*, *10*(9), 51–56. https://doi.org/10.17148/iarjset.2023.10907

Jain, M., Saihjpal, V., Singh, N., & Singh, S. B. (2022). *applied sciences An Overview of Variants and Advancements of PSO Algorithm*. 1–21.

Jangid, B. (2017). *Load flow Analysis using Backward Forward Sweep Method*. *Icaet*, 9–13.

Jani, A., & Makwana, V. H. (2018). *A Review on Shunt Compensating Devices for Reactive Power Management*. *5*(11), 26–34.

Kasari, P. R., Paul, M., Das, B., & Chakraborti, A. (2017). Analysis of D-STATCOM for power quality enhancement in distribution network. *IEEE Region 10 Annual International Conference, Proceedings/TENCON*, *2017-Decem*, 1421–1426. https://doi.org/10.1109/TENCON.2017.8228081

Katariya, C., & Shriwastava, R. (2016). Power Quality Improvement By Using D-STATCOM: Review. *IOSR Journal of Electrical and Electronics Engineering*, *2*(4), 2320–3331. www.iosrjournals.org

Kaur, S., & Gupta, S. (2021). *Importance of FACTS Devices in Power System*. *10*(12), 529–533. https://doi.org/10.21275/SR211207155622

Khalil, W. Al, Tanavade, S. S., Engineering, C., & Engineering, C. (2021). *APPLICATION OF STATIC VAR COMPENSATOR TO COMPENSATE REACTIVE POWER AND ENHANCE VOLTAGE PROFILE*. *12*(7), 23–31.

Mahdad, B. (2019). Optimal reconfiguration and reactive power planning based fractal search algorithm: A case study of the Algerian distribution electrical system. *Engineering Science and Technology, an International Journal*, *22*(1), 78–101. https://doi.org/10.1016/j.jestch.2018.08.013

Manoj, R. H., Kavita, S. G., & Jogi, V. (2017). Voltage regulation of STATCOM using flexible PI control. *Proceedings of the 2nd International Conference on Communication and Electronics Systems, ICCES 2017*, *2018-January*(March 2018), 128–133. https://doi.org/10.1109/CESYS.2017.8321248

Memon, S., Rahman, A., & Abbasi, S. (2017). *Analysis of Non-Technical Electrical Power Losses and their economic Impact on*. *June*.

Narain, A. (2015). *An Overview of Facts Devices used for Reactive Power Compensation Techniques*. *4*(12), 81–85.

Nascimento, S. Do, & Gouvêa, M. M. (2017). Voltage Stability Enhancement in Power Systems with Automatic Facts Device Allocation. *Energy Procedia*, *107*(September 2016), 60–67. https://doi.org/10.1016/j.egypro.2016.12.129

Niranjan, N., Manisha, & Sujata. (2016). Voltage Collapse: Causes and Prevention. *Voltage Collapse: Causes and Prevention*, *4*(02), 1–4.

Optimization, A., Algorithms, A. L. O., Merah, H., Gacem, A., Attous, D. Ben, Lashab, A., Jurado, F., & Sameh, M. A. (2022). *Sizing and Sitting of Static VAR Compensator (SVC) Using Hybrid Optimization of Combined Cuckoo Search (CS) and*.

Optimization, P. S. (n.d.). *16.4 Basic PSO Parameters*. 312–341.

Ouali, S., & Cherkaoui, A. (2020). *An Improved Backward / Forward Sweep Power Flow Method Based on a New Network Information Organization for Radial*. *2020*.

Philosophy, L. (2021). *DigitalCommons @ University of Nebraska - Lincoln Load Flow Solution of Distribution Systems - A Bibliometric Survey Load Flow Solution of*

Distribution Systems - A Bibliometric Survey. *July*.

Piotrowski, A. P., Napiorkowski, J. J., & Piotrowska, A. E. (2020). Population size in Particle Swarm Optimization. *Swarm and Evolutionary Computation*, *58*(March 2019), 100718. https://doi.org/10.1016/j.swevo.2020.100718

Prakash, P., & Khatod, D. K. (2016). Optimal sizing and siting techniques for distributed generation in distribution systems : A review. *Renewable and Sustainable Energy Reviews*, *57*, 111–130. https://doi.org/10.1016/j.rser.2015.12.099

Rehman, S., Khan, S. A., & Alhems, L. M. (2020). *The Effect of Acceleration Coefficients in Particle Swarm Optimization Algorithm with Application to Wind Farm Layout Design*. 922–930. https://doi.org/10.5937/fme2004922R

Reports, E. (2018). *Enhancement of voltage profile by incorporation of SVC in power system networks by using optimal load flow method in MATLAB / Simulink environments*.

Rosyadi, G., Syahputra, R., & Mujaahid, F. (2018). *Electrical Power Distribution Network Reliability : A Case Study in Wates Substation , Yogyakarta , Indonesia*. *2*(2), 52–58.

Sakthivel, S., Mary, D., & Kannan, V. S. (2016). *Optimal Location of SVC for Voltage Stability Enhancement under Contingency Condition through PSO Algorithm*. *20*(1), 30–36.

Salimon, S. A., Aderinko, H. A., & Damilola, F. I. (2019). *Load Flow Analysis of Nigerian Radial Distribution Network Using Backward / Forward Sweep Technique*. *2*(3), 1–11.

Shami, T. M., Mirjalili, S., Al-Eryani, Y., Daoudi, K., Izadi, S., & Abualigah, L. (2023). Velocity pausing particle swarm optimization: a novel variant for global optimization. In *Neural Computing and Applications* (Vol. 35, Issue 12). Springer London. https://doi.org/10.1007/s00521-022-08179-0

Shrivastava, C., Gupta, M., & Koshti, A. (2015). *Review of Forward & Backward Sweep Method for Load Flow Analysis of Radial Distribution System*. 5595–5599. https://doi.org/10.15662/ijareeie.2015.0406049

Singh, B., & Agrawal, G. (2018). Enhancement of voltage profile by incorporation of SVC in power system networks by using optimal load flow method in MATLAB/Simulink environments. *Energy Reports*, *4*, 418–434. https://doi.org/10.1016/j.egyr.2018.07.004

Song, Y., Hill, D. J., & Liu, T. (2020). Network-based analysis of rotor angle stability of power systems. In *Foundations and Trends in Electric Energy Systems* (Vol. 4, Issue 3). https://doi.org/10.1561/3100000011

Taktode, K. C., Rojatkar, G. S., Raut, B. T., & Nerkar, M. H. (2019). *Reactive Power Control by Using Thyristor Switched Capacitor (TSC) and Thyristor Controlled Reactor (TCR) in FACTS*. *8*(4), 61–64.

Terriche, Y., Su, C. L., Lashab, A., Mutarraf, M. U., Mehrzadi, M., Guerrero, J. M., & Vasquez, J. C. (2021). Effective Controls of Fixed Capacitor-Thyristor Controlled Reactors for Power Quality Improvement in Shipboard Microgrids. *IEEE Transactions on Industry Applications*, *57*(3), 2838–2849. https://doi.org/10.1109/TIA.2021.3058595

Turan, O., Sari, Y., & Koker, R. (2021). *Modelling a Static VAr Compensator consist of TCR and TSC TCR ve TSC ' den O luşan Bir Statik VAr Kompansatör Modellemesi*. *16*(1), 11–21.

Vairagade, P. P. (2017). *MARKET BASED POWER QUALITY IMPROVEMENT USING SERIES FACTS CONTROLLER SIMULATION*. *3*, 544–556.

Voltage, C., Index, S., Loss, L., Rate, R., Li, Z., Zou, Y., Gao, Z., Gong, J., Moghimi, S. M., Bostani, A., & Elahimanesh, A. (2019). *Effect of Inertia Weight of PSO on Optimal Placement of DG Effect of Inertia Weight of PSO on Optimal Placement of DG*. https://doi.org/10.1088/1757-899X/594/1/012011

Wang, D., Tan, D., & Liu, L. (2017). Particle swarm optimization algorithm : an overview. *Soft Computing*. https://doi.org/10.1007/s00500-016-2474-6

Woldu, T. A., Ziegler, C., & Wolter, M. (2020). A new method for prediction of static and dynamic voltage collapse using node parameters in large power networks. *IEEE PES Innovative Smart Grid Technologies Conference Europe*, *2020-October*, 344–348. https://doi.org/10.1109/ISGT-Europe47291.2020.9248887

Wondie, T. T. (2022). *Voltage Stability Assessments and Their Improvement Using Optimal Placed Static Synchronous Compensator (STATCOM). 2022*.

Yan, H., Jin, M. W., & Ping, Z. J. (2019). *The Parameters Selection of PSO Algorithm influencing On performance of Fault Diagnosis*. *02019*(2016), 1–5.

APPENDICES

Appendix -A: Interruption and Peak Load Data for Gefersa substation 15 KV Feeders

Table appendix-a:Two years (2015 and 2014) Interruption data of Gefersa Substation

Interruption data in 2014

Feder Name and pl	EEU Oromia Region 2014 SAIFI & SAIDI Report										Total Interruption	
	Permanent Fault				Temporary Fault				OP(Planned)			
	DPEF		DPSC		DTEF		DTSC					
	F	D [Hr.]	F	D [Hr.]	F	D [Hr.]	F	D [Hr.]	F	D [Hr.]	F	D(Hr)
L-1 4.36	8	70.5	10	48.25	11	0.5	12	1.5	19	22	60	142.75
L-3 4.25	11	55.5	10	48.9	10	0.9	5	1	16	35.5	52	141.8
L-5 3.6	5	30.2	3	8.5	2	0.8	0	0	9	20.8	19	59.98
L-6 3.54	6	22.5	7	15.8	7	0.7	8	0.53	11	18.8	39	58.33
L-11 3.58	5	25.57	12	50.72	6	0.52	1	0.25	15	14.7	39	91.76
L-12 4.08	13	31	14	38.5	9	0.6	3	0.15	20	45.6	59	115.85
L-13 3.93	4	28.5	15	55.6	11	0.8	5	0.5	14	25	49	110.4
L-14 4.45	15	65.3	15	77.5	14	1.5	5	2.5	16	26	63	172.8
L-8 3.77	1	1	0	0	4	0.25	0	0	11	10	16	11.25
L-9 3.75	2	3.5	0	0	3	0.15	0	0	2	5.5	7	9.15

Interruption data in 2015

Feder Name and pl	EEU Oromia Region 2015 SAIFI & SAIDI Report										Total Interruption	
	Permanent Fault				Temporary Fault				OP(Planned)			
	DPEF		DPSC		DTEF		DTSC					
	F	D [Hr.]	F	D [Hr.]	F	D [Hr.]	F	D [Hr.]	F	D [Hr.]	F	D(Hr)
L-1 3.875	9	71.73	11	49.43	10	0.8	10	1.25	20	23.15	60	146.37
L-3 3.58	10	55.58	11	47.93	12	0.88	4	0.33	17	35.95	54	140.68
L-5 3.52	5	28.2	4	8.83	1	0.08	0	0	8	18.58	18	55.7
L-6 3.41	5	22.78	6	13.08	8	0.6	7	0.43	10	19.78	36	56.68
L-11 3.66	4	24.67	13	49.72	5	0.42	3	0.23	16	13.77	41	88.8
L-12 4.28	14	32.1	15	39.65	8	0.63	2	0.17	21	46.62	60	119.17
L-13 4.208	3	29.85	16	53.67	10	0.92	4	0.33	15	26	48	110.77
L-14 4.58	15	67.3	16	79.55	14	1.05	2	0.5	15	27	62	175.4
L-8 3.355	0	0	0	0	3	0.25	0	0	10	9.43	13	9.68
L-9 3.25	1	2.78	0	0	2	0.17	0	0	1	4.67	4	7.62

Appendix-B: Standard conductor type and impedance per km

Table appendix-b: Cable type, resistance and reactance per km

Conductor Name (Size)	Resistance Per Km	Reactance Per Km
CU-20	1.426	0.396
AAC-25	1.338	0.380
ACSR-30	1.139	0.372
CU-25	0.936	0.387
ACSR-46	0.681	0.365
AAC-50	**0.680**	**0.362**
CU-35	0.659	0.374
ACSR-65	0.571	0.349
AAC-95	**0.58**	**0.341**
AAAC150	0.339	0.337
UGAL120	0.325	0.097
ACSR-129	0.291	0.317
AAAC-157	0.230	0.309
UGCU-120	0.196	0.097
AAAC-200	0.164	0.332

Appendix-C: EEU Energy Tariff

Table appendix-c: Energy tariff of the ethiopia electric utility

Tariff Type		As of Dec. 18 onward	As of Dec. 19 onward	As of Dec. 20 onward	As of Dec. 21 onward
Tariff Category	kwh/month	Birr/kwh	Birr/kwh	Birr/kwh	Birr/kwh
1.Residential tariff block					
1.1 1st block	Up to 50kwh	0.2730	0.2730	0.2730	0.2730
1.2 2nd block	Up to100kwh	0.4591	0.5617	0.6644	0.7670
1.3 3rd block	Up to 200kwh	0.7807	1.0622	1.3436	1.6250
1.4 4th block	Upto300kwh	0.9125	1.2750	1.6375	2.0000
1.5 5th block	Upto400 kwh	0.9750	1.3833	1.7917	2.2000
1.6 6th block	Upto500kwh	1.0423	1.4965	1.9508	2.4050
1.7 7th block	Above500kwh	1.1410	1.5877	2.0343	2.4810
2. General Tariff					
2.1 Flat Rate		1.0352	1.3982	1.7611	2.1240
3. Low Voltage Industry Tariff					
3.1 Flat Rate		0.8161	1.0544	1.2927	1.5310
3.2 Demand Charge rate		50.00	100.00	150.00	200.00
4. Medium Voltage Industry Tariff. 15kv & 33kv					
4.1 Flat Rate		0.6047	0.8008	0.9969	1.1930
4.2 Demand Charge rate		36.885	73.770	110.655	147.540
5. High Voltage Industry Tariff. Above 66kv					
5.1 Flat Rate		0.5174	0.6540	0.7911	0.9280
5.2 Demand Charge rate		21.9100	43.8200	65.7300	87.6400
6. Street Light Tariff					
6.1 Flat Rate		1.0352	1.3982	1.7611	2.1240
7. Bulk Supply Tariff					
7.1 Demand Charge rate per kw		39.2908	78.5815	117.872	157.160
7.2 Generation Tariff. Monthly per kwh		0.2218	0.4435	0.6653	0.8870

Appendix-D: Line and Load data for Gefersa 14 feeder

Table appendix-d: Line and load data of Gefersa 14-feeder

Branch No	From Bus	To Bus	Length	Conductor Type	R(Ω)	X(Ω)	KW	KVr
1	1	2	451.45	AAC-95	0.26183984	0.153943768	0	0
2	2	3	461.75	AAC-95	0.26781558	0.157457091	0	0
3	3	4	267.68	AAC-95	0.15525556	0.091279562	0	0
4	4	5	210.75	AAC-95	0.12223674	0.071866773	0	0
5	5	6	319.52	AAC-95	0.18532218	0.108956661	0	0
6	5	7	54.404	AAC-95	0.03155432	0.018551764	0	0
7	7	8	226.31	AAC-95	0.13126038	0.077172051	180	87.17797887
8	8	9	6.117	AAC-95	0.00354786	0.002085897	283.5	137.3053167
9	8	10	20.243	AAC-95	0.01174094	0.006902863	283.5	137.3053167
10	10	11	106.63	AAC-95	0.06184308	0.036359466	0	0
11	11	12	55.359	AAC-95	0.03210822	0.018877419	0	0
12	12	13	205.59	AAC-95	0.1192393	0.070104485	0	0
13	12	14	77.444	AAC-95	0.04491752	0.026408404	180	87.17797887
14	14	15	382.39	AAC-95	0.2217833	0.130393285	0	0
15	15	16	713	AAC-95	0.41354	0.243133	0	0
16	16	17	30.601	AAC-95	0.01774858	0.010434941	567	274.6106334
17	17	18	34.94	AAC-95	0.0202652	0.01191454	0	0
18	18	19	196.4	AAC-95	0.11390968	0.066971036	567	274.6106334
19	19	20	322.56	AAC-95	0.18708712	0.109994324	0	0
20	20	21	134.5	AAC-95	0.07801	0.0458645	0	0
21	21	22	200.56	AAC-95	0.11632422	0.068390619	0	0
22	22	23	95.99	AAC-95	0.0556742	0.03273259	283.5	137.3053167
23	23	24	175819	AAC-95	101.97502	59.954279	180	87.17797887
24	24	25	309.88	AAC-95	0.17973098	0.105669421	0	0
25	24	26	726.55	AAC-95	0.421399	0.24775355	283.5	137.3053167
26	26	27	259.94	AAC-95	0.15076346	0.088638517	567	274.6106334
27	27	28	171.87	AAC-95	0.09968634	0.058608693	0	0
28	28	29	127.92	AAC-95	0.07419592	0.043622084	0	0
29	29	30	114.66	AAC-95	0.06650106	0.039098037	180	87.17797887
30	30	31	1200.1	AAC-95	0.69603132	0.409218414	0	0
31	2	32	509.91	AAC-95	0.34673744	0.184586696	567	274.6106334
32	32	33	218.4	AAC-50	0.14851336	0.079061524	0	0
33	33	34	81.687	AAC-50	0.05554716	0.029570694	283.5	137.3053167
34	34	35	10.11	AAC-50	0.0068748	0.00365982	567	274.6106334

35	35	36	223.49	AAC-50	0.15197252	0.080903018	0	0
36	36	37	11.988	AAC-50	0.00815184	0.004339656	720	348.7119155
37	37	38	218.4	AAC-50	0.1485086	0.07905899	0	0
38	32	39	320.79	AAC-50	0.21813516	0.116124894	180	87.17797887
39	39	40	11.088	AAC-50	0.00753984	0.004013856	1125	544.8623679
40	40	41	112.96	AAC-50	0.07681348	0.040891882	0	0
41	41	42	62.048	AAC-50	0.04219264	0.022461376	283.5	137.3053167
42	42	43	48.172	AAC-50	0.03275696	0.017438264	0	0
43	42	44	86.529	AAC-50	0.05883972	0.031323498	90	43.58898944
44	44	45	466.95	AAC-50	0.31752328	0.169034452	0	0
45	44	46	173.77	AAC-50	0.11816564	0.062905826	90	43.58898944
46	46	47	200.18	AAC-50	0.13611968	0.072463712	0	0
47	46	48	391.89	AAC-50	0.26648724	0.141865266	283.5	137.3053167
48	48	49	117.84	AAC-50	0.08013256	0.042658804	0	0
49	32	50	435.97	AAC-50	0.29646096	0.157821864	90	43.58898944
50	50	51	395.13	AAC-50	0.26869044	0.143038146	0	0
51	50	52	335.7	AAC-50	0.22827464	0.121522676	567	274.6106334
52	52	53	1039.6	AAC-50	0.70691168	0.376326512	0	0
53	53	54	861.2	AAC-50	0.58561872	0.311755848	283.5	137.3053167
54	54	55	541.13	AAC-50	0.367965	0.19588725	283.5	137.3053167
55	55	56	226.66	AAC-50	0.15412948	0.082051282	567	274.6106334
56	56	57	217.7	AAC-50	0.14803464	0.078806676	0	0
57	56	58	324.23	AAC-50	0.2204764	0.11737126	567	274.6106334
58	37	59	165.18	AAC-50	0.11232104	0.059794436	22.5	10.89724736
59	59	60	83.714	AAC-50	0.05692552	0.030304468	283.5	137.3053167
60	40	61	73.99	AAC-50	0.0503132	0.02678438	45	21.79449472
61	61	62	41.78	AAC-50	0.0284104	0.01512436	180	87.17797887
62	62	63	36.673	AAC-50	0.02493764	0.013275626	0	0
63	52	64	268.04	AAC-50	0.18226448	0.097029032	283.5	137.3053167
64	64	65	56.976	AAC-50	0.03874368	0.020625312	0	0
65	4	66	57.056	AAC-50	0.03879808	0.020654272	45	21.79449472
66	66	67	154.5	AAC-50	0.10506204	0.055930086	0	0
67	66	68	131.9	AAC-50	0.08969472	0.047749248	283.5	137.3053167
68	68	69	52.879	AAC-50	0.03595772	0.019142198	0	0
69	11	70	200.93	AAC-50	0.136629	0.07273485	90	43.58898944
70	70	71	3108	AAC-50	2.11344	1.125096	0	0
71	14	72	222.49	AAC-50	0.15129184	0.080540656	90	43.58898944
72	72	73	64.108	AAC-50	0.04359344	0.023207096	0	0
73	15	74	1235.4	AAC-50	0.84009308	0.447226022	90	43.58898944
74	74	75	435.82	AAC-50	0.29636032	0.157768288	22.5	10.89724736
75	75	76	402.76	AAC-50	0.27387476	0.145798034	0	0
76	75	77	754.29	AAC-50	0.51291516	0.273051894	283.5	137.3053167
77	17	78	395.55	AAC-50	0.26897196	0.143188014	22.5	10.89724736

78	78	79	186.2	AAC-50	0.12661532	0.067404038	283.5	137.3053167
79	79	80	216.21	AAC-50	0.14702144	0.078267296	0	0
80	80	81	41.477	AAC-50	0.02820436	0.015014674	0	0
81	20	82	328.94	AAC-50	0.22367988	0.119076642	180	87.17797887
82	82	83	32.712	AAC-50	0.02224416	0.011841744	283.5	137.3053167
83	83	84	112.54	AAC-50	0.07652516	0.040738394	0	0
84	84	85	66.316	AAC-50	0.04509488	0.024006392	0	0
85	21	86	130.25	AAC-50	0.08857136	0.047151224	180	87.17797887
86	86	87	66.661	AAC-50	0.04532948	0.024131282	283.5	137.3053167
87	87	88	50.953	AAC-50	0.03464804	0.018444986	0	0
88	87	89	23.263	AAC-50	0.01581884	0.008421206	283.5	137.3053167
89	89	90	56.658	AAC-50	0.03852744	0.020510196	0	0
90	89	91	332.58	AAC-50	0.226151	0.12039215	283.5	137.3053167
91	91	92	7.257	AAC-50	0.00493476	0.002627034	0	0
92	27	93	352.76	AAC-50	0.23987408	0.127697672	45	21.79449472
93	93	94	96.498	AAC-50	0.06561864	0.034932276	0	0
94	93	95	40.773	AAC-50	0.02772564	0.014759826	180	87.17797887
95	28	96	450.86	AAC-50	0.3065814	0.16320951	22.5	10.89724736
96	96	97	256.74	AAC-50	0.17458184	0.092939156	283.5	137.3053167
97	97	98	28.166	AAC-50	0.01915288	0.010196092	0	0
98	30	99	320.51	AAC-50	0.21794544	0.116023896	45	21.79449472
99	99	100	278.79	AAC-50	0.18957856	0.100922704	0	0
100	99	101	259.54	AAC-50	0.17648448	0.093952032	90	43.58898944
101	101	102	169.95	AAC-50	0.11556804	0.061522986	0	0
102	101	103	121.47	AAC-50	0.0825962	0.04397033	45	21.79449472

Appendix-E: Sample Matlab Code of the thesis

```
clc
clear all
close all
%% SVC size minimum and maximum value
no_of_SVC=1;
svc_size_min=10;
svc_size_max=1000;
voltage_minimum=0.95;
voltage_maximum=1.0;
current_maximum=2000;
nbus=103;
no_of_int_pop=10;
no_of_iter=1000;
%%
data_pass_to_loadflow{2}=voltage_minimum;
data_pass_to_loadflow{3}=voltage_maximum;
data_pass_to_loadflow{4}=vcurrent_maximum;
data_pass_to_loadfflow{12}=no_of_SVC;
%% apply load flow base case
[objective_result]=load_flow_process_basecase(nbus,data_pass_to_loadflow);
```

```
power_loss_base_case=objective_result{1};
voltage_base_case=objective_result{4};
%% only svc
for km=2:33
    min_val1=km;
    max_val1=km;
    min_val2=svc_size_min;
    max_val2=svc_size_max;
    data_pass_to_loadflow{12}=1;
    no_in_val=1;
    %% pso algorithm process

[data_final_pso,final_fit_pso]=pso_process_dgplace(nbus,no_of_int_pop,...
       no_of_iter,min_val1,max_val1,min_val2,max_val2,...
       no_in_val*2,data_pass_to_loadflow);
   Final_svc_loc=data_final_pso;
   svc_location=Final_svc_loc(1:no_of_svc)
   svc_size_KW=Final_svc_loc(no_of_svc+1:end)
   [objective_result]=load_flow_process_withdg(nbus,...
       Final_svc_loc,data_pass_to_loadflow);
   power_loss_P=objective_result{1};power_loss_Q=objective_result{3};
   line_loss_P=objective_result{5};voltage_with_svc=objective_result{4};
   %% plot loss and voltage graph
   figure,bar(1:length(line_loss_p),line_loss_p);
   xlabel('line number');ylabel('real power loss');grid on;
   title('power of a 33-bus test system');
   figure, plot(1:length(voltage_base_case), voltage_base_case,'r-
s','linewidth',2);
   hold on; plot(1:length(voltage_with_svc),voltage_with_svc,'b-
s','linewidth',2);
   xlabel('bus number'); ylabel('bus voltage');grid on;
   title('voltage profile pso algorithm');
   legend('with out svc',['with',num2str(no_of_svc),'svc']);
```